In search for potential antidiabetic compounds from natural sources: docking, synthesis and biological screening of small molecules from Lycium spp. (Goji)

Chinni Yalamanchili
University of Mississippi

Amar G. Chittiboyina
University of Mississippi School of Pharmacy

Saqlain Haider
University of Mississippi School of Pharmacy

Yelkaira Vasquez
University of Mississippi

Shabana Khan
University of Mississippi

See next page for additional authors

Recommended Citation

Yalamanchili, C., Chittiboyina, A. G., Haider, S., Vasquez, Y., Khan, S., do Carmo, J. M., da Silva, A. A., Pinkerton, M., Hall, J. E., Walker, L. A., & Khan, I. A. (2020). In search for potential antidiabetic compounds from natural sources: docking, synthesis and biological screening of small molecules from Lycium spp. (Goji). Heliyon, 6(1), e02782. https://doi.org/10.1016/j.heliyon.2019.e02782

Authors

Chinni Yalamanchili, Amar G. Chittiboyina, Saqlain Haider, Yelkaira Vasquez, Shabana Khan, Jussara M. do Carmo, Alexandre A. da Silva, Mark Pinkerton, John E. Hall, Larry A. Walker, and Ikhlas A. Khan

Research article

In search for potential antidiabetic compounds from natural sources: docking, synthesis and biological screening of small molecules from *Lycium spp.* (Goji)

Chinni Yalamanchili [a], Amar G. Chittiboyina [b,*], Saqlain Haider [b], Yelkaira Vasquez [a], Shabana Khan [a,b], Jussara M. do Carmo [c,d], Alexandre A. da Silva [c,d], Mark Pinkerton [c,d], John E. Hall [c,d], Larry A. Walker [b], Ikhlas A. Khan [a,b]

[a] *Divison of Pharmacognosy, Department of BioMolecular Sciences, School of Pharmacy, The University of Mississippi, University, MS, 38677, USA*
[b] *National Center for Natural Products Research; School of Pharmacy, The University of Mississippi, University, MS, 38677, USA*
[c] *Department of Physiology and Biophysics, The University of Mississippi Medical Center, 2500 N. State St. Jackson, MS, 39216, USA*
[d] *Mississippi Center for Obesity Research, The University of Mississippi Medical Center, 2500 N. State St. Jackson, MS, 39216, USA*

A R T I C L E   I N F O

A B S T R A C T

Current clinical antidiabetic drugs, like rosiglitazone **1**, have been implicated in some serious side effects like edema, weight gain, and heart failure, making it necessary to find alternative agents. Partial agonists of peroxisome-proliferator activated receptor-gamma (PPARγ) were determined to possess improved insulin sensitivity without undeseirable side-effects when compared to full agonists of PPARγ, like rosiglitazone **1**. The traditional Chinese medicine (TCM) plants, Goji (*Lycium barbarum* and *Lycium chinense*) are widely used for treating symptoms related to various diseases including diabetes and hypertension. Twenty-seven reported compounds from Goji were docked into both partial- and full-agonist binding sites of PPARγ. Amongst the docked compounds, phenylethylamide-based phytochemicals (**5–9**) (termed as tyramine-derivatives, TDs) were found to possess good docking scores and binding poses with favorable interactions. Synthesis of 24 TDs, including three naturally occuring amides (**6, 8, 9**) were synthesized and tested for PPARγ gene induction with cell-based assay. Three compounds showed similar or higher fold induction than the positive control, rosiglitazone. Among these three active TDs, *trans-N*-feruloyloctopamine (**9**) and tyramine derivatives-enriched extract (**TEE**) (21%) of the root bark of *L. chinense* were further studied *in vivo* using db/db mice. However, both **TEE** as well as **9** did not show significant antidiabetic properties in db/db mice. *In vivo* results suggest that the proposed antidiabetic property of *Lycium* species may not be due to tyramine derivatives alone. Further studies of tyramine derivatives or enriched extract(s) for other bioactivities like hypocholesterolemic activities, and studies of novel isolated compounds from Goji will enable a more complete understanding of their bioactivities.

1. Introduction

Type 2 diabetes mellitus (T2DM), a disorder resulting from insulin resistance and impaired pancreatic beta cell function, has reached epidemic proportion and is responsible for 1.5 to 5.5 million deaths per year in 2012 and 2013, worldwide. As per World Health Organization (WHO) statistics, T2DM accounts for about 90% of the total diabetic populations of 382 million, which was 8.3% of the total adult population in 2012–2013 [1]. According to the American Diabetes Association, there are approximately 1.5 million new cases of diabetes each year and, if the

current trend continues, these numbers are projected to increase to a third of the population by 2050 [2]. Alarmingly, patients with impaired glucose and lipid metabolisms have increased risk of developing complications such as dyslipidemia, hypertension, and other adverse cardiovascular effects. Current antidiabetic drugs include: metformin (biguanide), which reduces gluconeogenesis; sulfonyl ureas (gliburide, glipizide, glimpiride), which are insulin secretagogues; competitive α-glucosidase inhibitors (acarbose, miglitilol); and thiazolidinediones (TZDs) which include rosiglitazone **1** (Avandia®) and pioglitazone (Actos®) are effective in improving insulin and glucose parameters and

increase whole-body insulin sensitivity [3]. TZDs decrease hepatic glucose production and prolong pancreatic β-cell function by preventing apoptosis of β-cells [3]. TZDs exert their action by acting as agonists to nuclear receptor peroxisome proliferator-activated receptor subtype gamma (PPARγ). The structure of apo-PPARγ site along with co-activating factor SRC-1 was determined (PDB: 2PRG) (Supplementary information, SI Figure A.1) [4]. Depending on their interaction with the key residues in the ligand binding domain of PPARγ, there are two binding modes of PPARγ agonists: full-agonist and partial-agonist (Supplementary information, SI Figure A.2). Although TZDs are useful in treating T2DM, adverse effects like weight-gain, edema, and anemia are often observed with full agonists like rosiglitazone 1 and the treated populations have increased risk for cardiovascular events and bone fracture [5]. The other adverse side effects associated with rosiglitazone include congestive heart failure, volume-overload, systemic edema due to fluid retention and subsequent increase in intravascular volume [3]. The partial agonists like cercosporamide [6, 7, 8, 9, 10] (Fig. 1) improve insulin sensitivity without causing undesirable side-effects associated with full agonists like TZDs [11,12] and interact differently at the PPARγ binding site. In addition to antidiabetic properties, PPARγ agonists have been shown to exhibit pleiotropic beneficial effects in addition to its blood glucose-lowering effects. These include effects on vasculature, lowering of blood pressure, preventing the progression of atherosclerosis, and reno-protective effects by reducing the urinary albumin in both human and animals [13].

Several natural products have been reported to possess PPARγ activities with reduced side-effects compared to TZDs [8,14, 15, 16, 17, 18] and bind with PPARγ binding pocket in a manner different from full agonists. We hypothesize that small molecules isolated from traditionally used plants could possess PPARγ activities with reduced side-effects compared to TZDs. Our objectives were to apply computational methods for the identification of potential PPARγ modulators, validate with cell-based methods and confirm the preliminary results with animal models. Plants such as *Lycium barbarum* and *L. chinense*, also known as *gou qi zi* or Goji, wolfberry, Chinese wolfberry or matrimony wine, have been widely used in Asian countries for the treatment of a number of

symptoms related to [12, 19] diabetes, inflammation and as a tonic for well-being. The phytochemicals reported from Goji were claimed to exhibit antioxidant, antitumor, immunomodulatory, cardioprotective, antidiabetic and neuroprotective activities [19, 20, 21, 22, 23, 24, 25, 26, 27, 28, 29, 30, 31, 32]. The dried root bark of *L. barbarum*, has been shown to produce long-term hypoglycemic effects and reduced body weight in diabetic mice [23]. Methanolic extracts made from the root bark of *L. chinense* were claimed to possess hypocholesterolemic and antioxidant effects [33]. In order to identify novel PPARγ modulators with reduced side-effects, for the treatment of T2DM, we carried out this study in four parts.

Stage 1: Docking studies to identify the reported phytochemicals of Goji which occupy the same chemical space as that of the known agonist and partial agonist binding pockets of PPARγ.

Stage 2: Synthesis of naturally occurring phenethylamides and related analogs.

Stage 3: *In vitro* screening of tyramine-like compounds for PPARγ/ PPARα agonistic activity.

Stage 4: *In vivo* study of a small molecule and phenethylamides-enriched extract for antidiabetic activity, with db/db mice.

2. Results and discussion

Twenty-seven reported- (at the time of our study) phytochemicals isolated from various parts of Goji (*L. barbarum* and *L. chinense*), were selected for the docking studies (Fig. 2). These include terpenes, tyramine-based phenethylamides, amide derivatives, N-methyl calystegines, pyrrole analogs, cyclic peptides and glycosides.

2.1. In silico molecular docking

Both the partial- and full- agonist binding sites of PPARγ were utilized for docking studies. Partial- and full- agonists possess dissimilar binding modes by possessing variable ligand-residue interactions. While full agonists (rosiglitazone 1, PDB: 2PRG) show good hydrogen bonding interactions with His343 on helix 4, His449 on helix 10, and Tyr473 on
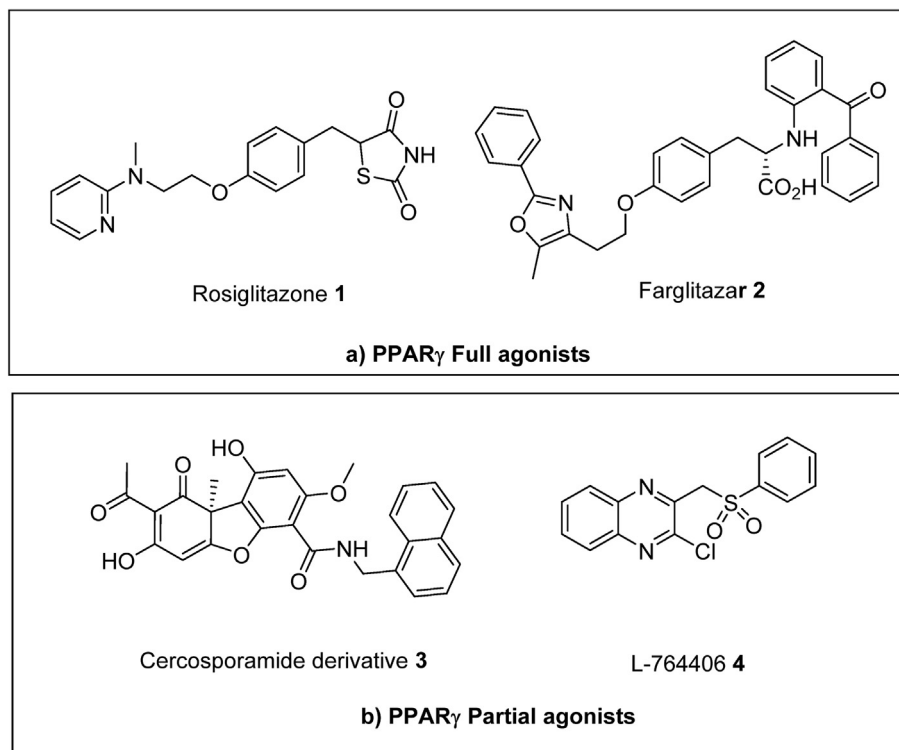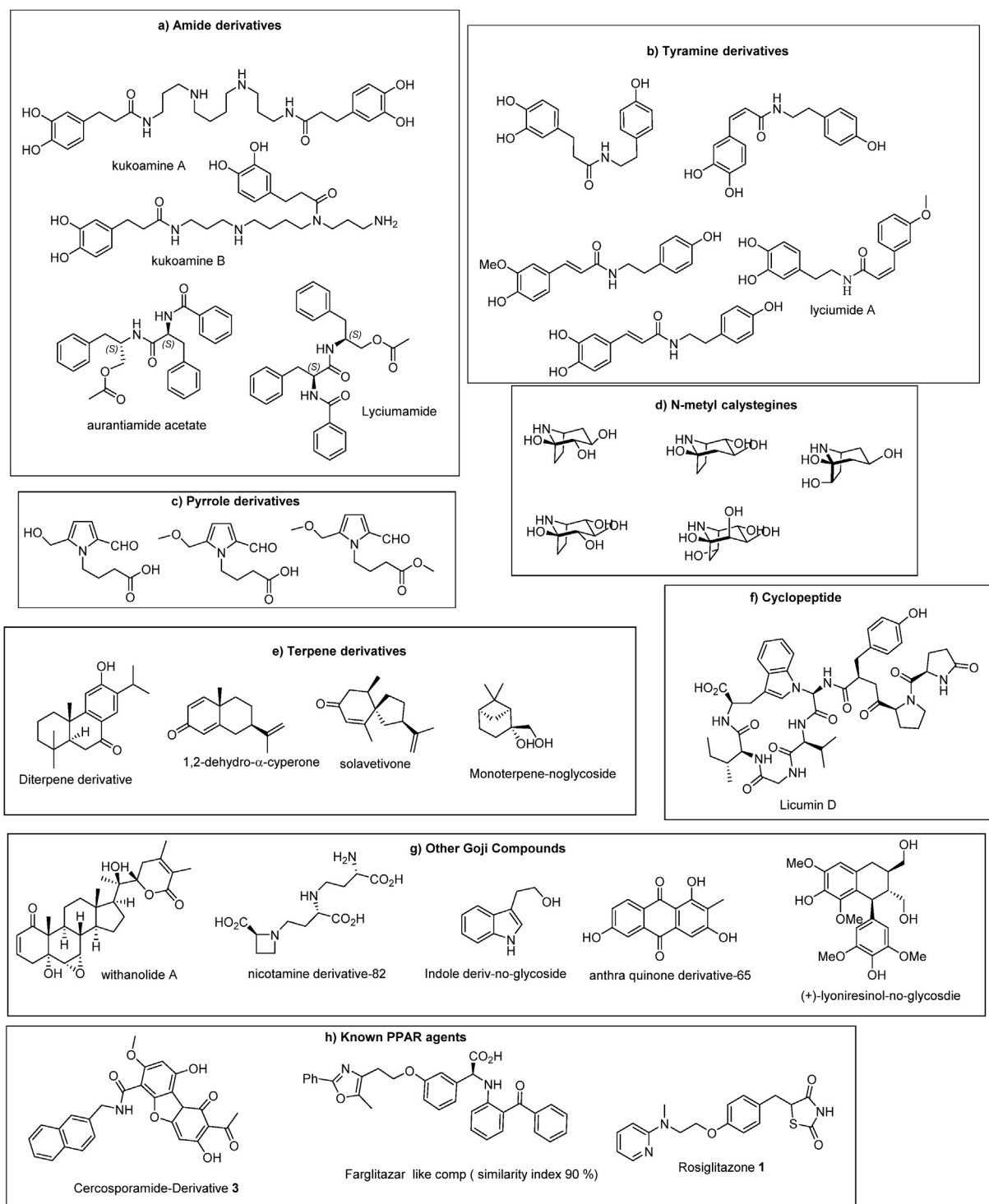

Fig. 1. Types of PPARγ ligands. a) Full agonists: Rosiglitazone 1 and Farglitazar 2; b) Partial agonists: Cercosporamide-derivative 3 and L-764406 4.

Fig. 2. List of the compounds used for docking studies in PPARγ crystal structures PDB ID: 2PRG (Rosiglitazone **1**), 3LMP (Cercosporamide-derivative **3**). a) Amide derivatives, b) Tyramine derivatives, c) Pyrrole derivatives, d) N-methyl calystegines, e) Terpene derivatives, f) Cyclopeptide (Licumin D), g) other Goji compounds and h) known PPAR agents.

helix 12, partial agonists (Cercosporamide-derivative **3**, PDB: 3LMP) do not show any interactions with these residues. However, partial agonists occupy the binding site in the region between helix 3 and the β-sheet (Supplementary information, SI Figure A.2).

Using the X-ray crystal structures of both full agonist rosiglitazone **1** (PDB ID: 2PRG) and partial agonist, cercosporamide-derivative **3** (PDB ID: 3LMP) [12], docking was performed on the ligand binding domain of PPARγ using the twenty seven reported compounds isolated from various

parts of both *L. barbarum* and *L. chinense*. Grids were generated around the native ligand using the Glide SP module (Schrödinger, LLC) with 12 Å radii generated with different hydrogen bonding constraints for full (2PRG) and partial agonist (3LMP) crystal structures. For the full agonist crystal structure, 2PRG, three hydrogen-bonding constraints (His343 on helix 4, His449 on helix 10, and Tyr473 on helix 12) were applied, and in the partial agonist crystal structure, 3LMP, no constraints were applied. The output of docking in both partial- (3LMP) and full- agonist (2PRG)

binding sites were analyzed (Supplementary information, SI Tables 1 & 2) which revealed that several compounds possessed good binding poses with favorable protein-ligand interactions. A study of the binding modes and the docking scores revealed that five compounds possessed good binding poses, comparable to the native ligands. These compounds belonged to the cinnamomylphenethyl amide class (or phenyl-ethylamides) termed tyramine derivatives TDs, hereafter for simplicity: lyciumamide A **5**, dihydro-*N*-caffeoyltyramine **6**, *cis*-*N*-caffeoyltyramine **7**, *trans*-*N*-caffeoyltyramine **8**, *trans*-*N*-feruloyloctopamine **9** (Table 1).

TDs displayed binding poses similar to both full and partial agonists. They showed good hydrogen bonding interactions with the residues on the helix 3 and helix 12 (similar to the full agonist, rosiglitazone **1**), as well as occupying the region between helix 3 and β-sheet (mimicking the binding pose of the partial agonist, cercosporamide-derivative **3**), with no apparent interaction with AF2 helix binding site (Figs. 3 and 4). This
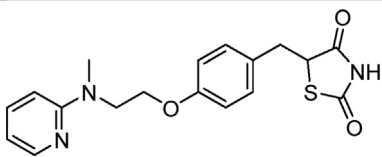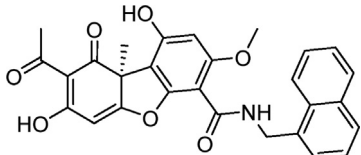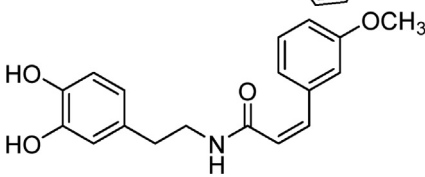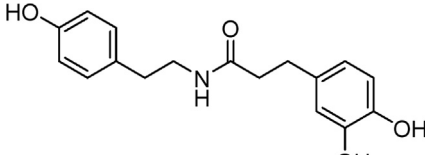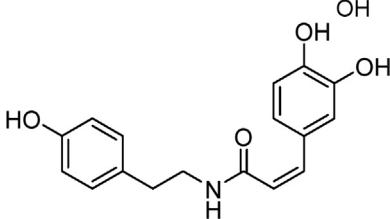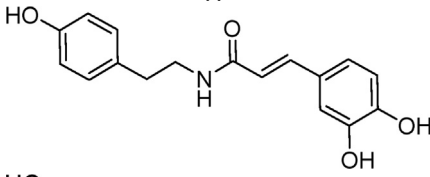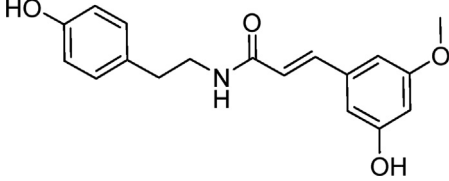
suggested that TDs are capable of occupying both binding domains with structural flexibility and may serve as a source of full and/or partial agonists for PPARγ. Some of the TDs were previously studied and re-ported to possess diverse biological activities including antitubercular activity [34], inhibitors of bacterial efflux pump, melanin synthesis [35], melanocyte-tyrosinase [36] and antifungal activities [37]. However, their antidiabetic potentials including modulation of PPARs were not reported. Recently, other types of tyramine derivatives were found to possess α-glucosidase inhibitory activity [38].

2.2. Synthesis of tyramine derivatives (TDs)

To test the validity of *in silico* results, twenty-four tyramine analogs (TDs) including three natural constituents of *L. chinense* (**6**, **8**, **9**) were synthesized *via* simple peptide coupling conditions [39]. Four readily

Table 1
Docking scores of the five tyramine-based secondary metabolites in full agonist and partial agonist binding sites of PPARγ.

Compound	Structure	Glide Docking Score	
		2PRG (Agonist)	3LMP (Partial agonist)
Rosiglitazone (**1**)		-11.68 (native ligand)	-9.10
Cercosporamide-derivative (**3**)		No docking result obtained	-10.11 (native ligand)
Lyciumamide A (**5**)		-8.36	-7.47
Dihydro-N-caffeoyltyramine (**6**)		-8.82	-8.10
cis-N-caffeoyltyramine (**7**)		-5.70	-6.26
trans-N-caffeoyltyramine (**8**)		-7.50	-6.16
trans-N-feruloyloctopamine (**9**)		-7.31	-8.11

Fig. 3. a) Docked poses of the five tyramine-based secondary metabolites in PPARγ crystal structure with rosiglitazone **1**, PDB: 2PRG. Tyramine derivatives- **5** (Brown), **6** (Blue), **7** (dark green), **8** (wheat), **9** (light green), Rosiglitazone **1** (yellow); key interacting residues in pink. b) Ligand-interaction diagram of **6** with key amino acid residues of PPARγ (PDB: 2PRG).

Fig. 4. a) Docked poses of the five tyramine-based secondary metabolites in PPARγ crystal structure with cercosporamide-derivative, PDB: 3LMP; **5** (dark blue), **6** (brown), **7** (light blue), **8** (black), **9** (light green), 3LMP-ligand **3**(green); key interacting residues in pink. b) Ligand-interaction diagram of **6** with key amino acid residues of PPARγ (PDB: 3LMP).

available cinnamic acids (**10** to **13**) were coupled with three readily available tyramines (**14** to **16**) in the presence of triethylamine and PyBOP [(benzotriazole-1-yloxy) tripyrrolidino-phosphoniumhexa-fluorophosphate] as an activator to produce twelve TDs **8, 9, 17–26**

which were further hydrogenated to their corresponding saturated analogs **6, 27–37** (Scheme 1). All the 24 TDs (**6, 8, 9, 17–37**) were screened with luciferase assays for agonistic activities towards both PPAR isoforms (Section 2.4).

Scheme 1. Synthesis of twenty-four tyramine derivatives. Reagents and conditions: a. PyBOP, TEA, DMF: DCM (1:1 v/v), 0 °C, 12h (57–83%); b. H_2 (1 atm) Pd/C, MeOH, 12h (49–90%).

2.3. Tyramine-enriched extract (TEE)

Four phenolic amides were previously reported to be isolated from the root barks of *L. chinense* including *dihydro-N*-caffeoyl tyramine **6** (106 mg, 0.01325%), *cis-N*-caffeoyl tyramine **7** (9.2 mg, 0.00115%), *trans-N*-caffeoyl tyramine **8** (14.8 mg, 0.00185), and *trans-N*-feruloyloctopamine **9** (19.6 mg, 0.00245%) [37, 40]. In order to study and compare the antidiabetic properties of newly prepared TDs along with extract, an enriched methanolic extract of the root bark of *L. chinense* (**TEE**) containing 21% (calculated amount based on the literature values) TDs was prepared to study in db/db mice.

2.4. In vitro PPAR luciferase assay

All the twenty-four synthesized tyramine derivatives were screened for *in vitro* activity using PPARγ, PPARα luciferase assays [41]. These compounds were screened for their selectivity towards PPARγ over PPARα at three different concentrations of 30, 10 and 3 µM, along with the known ligands rosiglitazone **1** (PPARγ agonist) and ciprofibrate (PPARα agonist). PPARγ and PPARα agonistic activities of the compounds were measured in terms of fold induction in luciferase expression compared to the DMSO control, with a two-fold induction meaning a 100% increase. Among the twenty-four compounds, three compounds **9**, **17** and **24** showed a considerable increase in PPARγ activity with a fold induction of 2.0, 2.1 and 1.5 at 30 µM, respectively. Under the similar experimental condition, rosiglitazone **1** showed an induction of 3.1 folds (Table 2). However, PPARα induction by the synthesized compounds was found to be negligible, showing the selective nature of these compounds towards PPARγ. Based on these results, **9** was selected for further studies with animal models.

2.5. In vivo testing in mice

Compound **9** and **TEE** (with ~21% tyramine derivatives) were tested *in vivo* using diabetic db/db mice. The dosage of **TEE** was established on the basis of the concentrations of tyramine-like compounds in the enriched extract. Several parameters were measured including body weight, food intake, glucose tolerance, metabolic data, body composition, blood pressure and heart rate for the mice treated with **9**, and **TEE** and the resulting data for the control vs treatment period at medium and high doses were assessed. Rosiglitazone **1** is an FDA approved drug, hence, it was not included in our animal studies.

2.5.1. Body weight, food intake and glucose tolerance measurements

Body weight and food intake of both high- and medium-dose db/db mice groups were measured during the two weeks of control-period and during the 18-day period of treatment with compound **9**, **TEE** or vehicle. In the high-dose groups, the mice treated with **9** showed a slight increase in body weight, whereas, the group treated with **TEE** showed a slight decrease in their body weight. The medium-dose group mice treated with **TEE** and **9** showed a slight decrease in body weight (Fig. 5). The food intake of high-dose groups treated with **9** increased, while that of the **TEE**-treated group decreased slightly. In the medium-dose group treated with the **TEE**, the food intake decreased slightly, whereas the mice treated with the drug remained the same (Fig. 5).

Table 2
PPARγ activation by compounds **9**, **17** & **24**.

Compound	Fold induction of PPAR gamma activity		
	30 µM	10 µM	3 µM
9	2.0 ± 0.16	1.9 ± 0.01	1.4 ± 0.13
17	2.1 ± 0.04	1.4 ± 0.09	1.4 ± 0.17
24	1.5 ± 0.24	0.9 ± 0.02	1.0 ± 0.15
Rosiglitazone*	3.1 ± 0.10	2.5 ± 0.05	2.1 ± 0.20

* Positive control.

Glucose tolerance tests were performed in the mice treated with the high- and medium-doses of the **TEE** and **9**. In both medium- and high-dose treated groups, no improvement was observed in baseline glucose or in glucose tolerance in the mice treated with **9** or **TEE**. The data for glucose tolerance in the medium and high dosage groups is shown in the Fig. 6.

2.5.1.1. Metabolic data.
Data related to respiratory quotient (RQ), oxygen consumption (VO$_2$), carbon dioxide production (VCO$_2$), heat production, and total movement were measured in both the medium- and high-dose groups (Fig. 7a and b). In the medium-dose group treated with **9**, the respiratory quotient, VO$_2$, VCO$_2$ decreased significantly, whereas, the heat production decreased slightly and motor activity increased slightly compared to the baseline. In the **TEE** treated medium-dose group, all the metabolic parameters decreased slightly compared to the baseline.

In the high-dose group mice treated with **9**, the respiratory quotient and total average movement decreased, while VO$_2$, VCO$_2$ and heat production increased. In the **TEE** treated high-dose group, the respiratory quotient decreased slightly, the total average motor activity increased significantly, whereas, VO$_2$, VCO$_2$ remained the same and the heat production decreased (Fig. 8a and b). However, these observed changes appear to be not statistically significant.

2.5.1.2. EchoMRI body composition.
Body composition was measured in the medium-dose group using EchoMRI to assess lean and fat mass, free and total water content (Fig. 9). In the drug-treated mice, lean mass, fat mass and total water content almost remained the same as the baseline, free-water content decreased by 42% in the first week, and it slightly increased in the second week. In the **TEE**-treated group, the lean mass remained the same, fat mass slightly increased by 5% in the first and second weeks, and free-water content increased by 8% in the first week and returned back to baseline in the second week.

2.5.1.3. Blood pressure and heart rate.
Heart rate and blood pressure were measured in the high-dose group after treatment with **TEE** and compound **9**. The heart rate of the mice (Fig. 10) slightly increased in both **9** and **TEE** treated mice. The blood pressure in the high-dose group of mice (Fig. 11) treated with the **9** slightly decreased, whereas, with the **TEE**, the blood pressure slightly increased.

Based on the *in vivo* results, it can be inferred that the tyramine derivative **9** and the enriched extract **TEE**, do not possess significant antidiabetic activities. However, it should be noted that several novel phytochemicals were later reported (and not included in these docking studies) to be isolated form Goji and were reported to possess myriad of bioactivities including activities against Alzheimer's disease with lycibarbarsermidines A–O, dicaffeoylspermidine derivatives [29].

Four new phenolic amides along with thirteen known phenolic amides were identified recently from the stem of *Lycium barbarum* and were evaluated against human glioma stem cell lines and two compounds grossamide and 4-O-methylgrossamide were found to possess moderate cytotoxicity [31].

In a randomized, double-blinded placebo-controlled trial, dietary wolfberry extract was reported to modify oxidative stress by controlling the expression of inflammatory mRNAs with slight but significant decrease in erythrocyte superoxide dismutase activity and increase in catalase activity [26]. This indicates that TDs could possibly be acting on non-PPARγ dependent biological targets to possess antiinflammatory and hypocholesterolemic activities. Further studies on these TDs, including possible combination effects, will enable our understandings on their overall bioactivity including multi-drug targets [42] to explain their PPARγ-like anticancer and antiinflammatory activities.
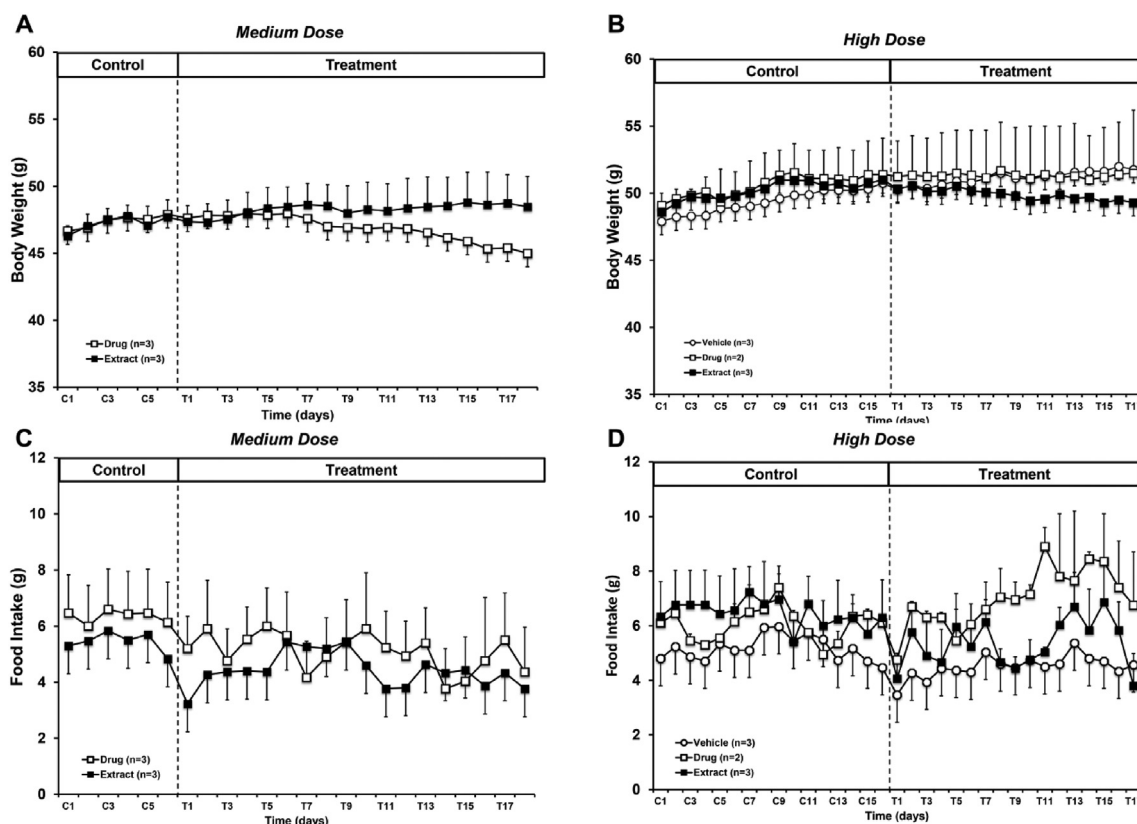
Fig. 5. Body weight (A, B) and food intake (C, D) by db/db mice in both high- and medium-dose group, treated with **9** and **TEE** (enriched with tyramine-based amides).

3. Conclusion

Preparations containing Goji, a traditional Chinese medicine (TCM) plant, are widely used in the Eastern countries to treat various symptoms including diabetes. To identify the active compounds, the reported phytochemicals of Goji were selected and docked into the PPARγ ligand binding domains of both full and partial agonists (2PRG and 3LMP, respectively). Docking results revealed that five compounds belonging to cinnamomylphenethyl amide class (**5**–**9**) (termed tyramine-derivatives) (TDs), possess good binding poses and docking scores in both the partial and full agonist binding domains. Hence, tyramine-derivatives were selected for the synthesis followed by their further testing in cell-based as well as animal models. A tyramine enriched extract **TEE** from the root bark of *L. chinense* was prepared. Using a coupling reaction of phenethylamine with cinnamic acid-derivatives, followed by reduction, twenty-four compounds belonging to the tyramine-derivatives were synthesized, evaluated for PPARγ activity and selectivity using PPARγ- and PPARα-luciferase bioassays. Among the twenty-four compounds, three compounds (**9**, **17**, and **24**) possessed a good induction of PPARγ compared to the positive control, rosiglitazone **1** and selectivity over PPARα isoform.

To validate the *in vitro* data further, compound **9** and tyramine-derivative enriched **TEE** were tested using *in vivo* diabetic db/db mice to check their antidiabetic and metabolic properties. Although some tyramine derivatives possessed good activities *in vitro*, the results of the *in vivo* studies indicate no significant improvement in the biochemical parameters in db/db mice model for both **9** and tyramine-derivative enriched Goji fraction.

In summary, though Goji has been reported and used for their antidiabetic properties as per TCM, our studies indicate that this antidiabetic property may not be due to the TD-class of compounds either standalone or in the enriched extract **TEE**, at the tested concentrations *in vivo*. It is plausible that the phytochemicals of Goji including tyramine-analogs might be working as antidiabetic compounds *via* different targets or mechanisms other than activation of PPARγ or could possess other relevant biological activities like hypocholesterolemic activities.

4. Experimental

4.1. Docking studies

Docking studies were performed using a commercial version of the Schrödinger software package [43] installed on a Windows desktop computer with Intel® Core™ Quad CUP Q6600@2.40GHz 2.40 GHz processor with a random access memory (RAM) of 4.00 GB and 32-bit operating system. PyMol software (Schrödinger, LLC) was utilized to perform post docking visualization and analysis.

4.1.1. Protein preparation

Crystal structures of PPARγ with rosiglitazone **1**, a full agonist (PDB: 2PRG) and cercosporamide-derivative **3**, a partial agonist (PDB: 3LMP) were prepared using the protein preparation wizard. Both the proteins were preprocessed to assign bond orders, add hydrogen bonds, create zero-order bonds to metals, create disulfide bonds, and delete water molecules beyond 5 Å from the hetero groups. For 2PRG, the chains B and C were deleted, whereas, for 3LMP, chain C was deleted. The H-bond assignment was applied using sample water orientations, using PROPKA pH 7.0. Water molecules with less than three hydrogen bonding distance were removed from the protein. Restrained minimization was performed using OPLS_2005, converged the heavy atoms to RMSD 0.3 Å.

4.1.2. Ligand preparation

Thirty compounds, including 27 from Goji and three PPARγ agonist ligands like farglitzar, rosiglitazone **1** and cercosporamide-derivative **3**
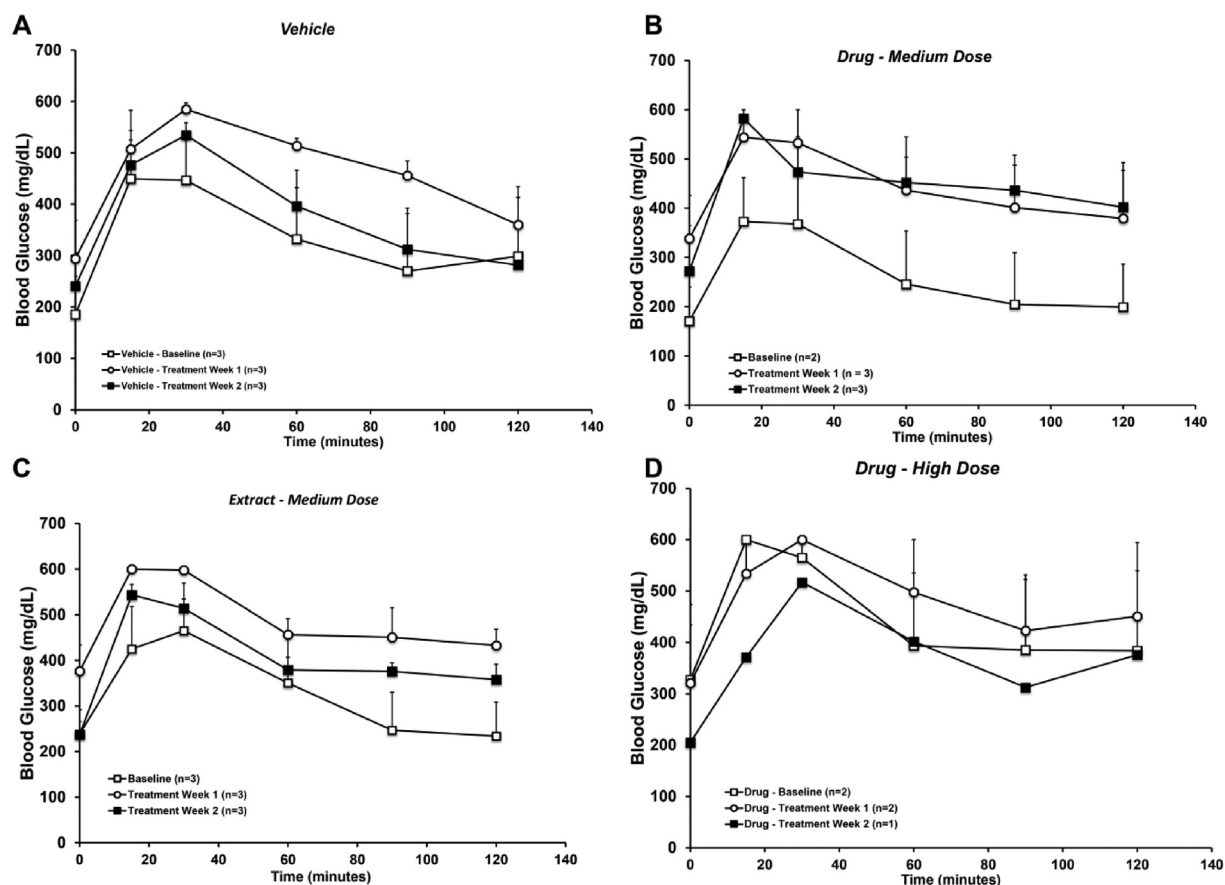
Fig. 6. Blood glucose measurements plotted against time for **TEE** and compound **9** in (A) vehicle, medium (B, C) and high dosage (D) of the db/db mice (n = 3).

were prepared using LipPrep module (Schrödinger, LLC) in OPLS-2005 force field, ionized at pH 7.4 ± 2, desalted and generated tautomers. The specified chirality was retained to generate at most 32 per ligand. This ligand preparation generated 81 ligands from the input of 30 compounds.

4.1.3. Glide grid generation and docking

Receptor grids were generated for the prepared proteins 2PRG and 3LMP using Glide (Schrödinger, LLC). For 2PRG, three hydrogen bonding constraints to His323, His449 and Tyr473 were applied, and for 3LMP, no constraints were applied. The grids thus generated were validated for both the native ligands to check if the RMSD of the docked output was <1 Å from that of the crystal structure. All the prepared ligands were docked in the two generated grids. Their docking results and binding poses were analyzed using PyMol (Schrödinger, LLC). The docking output of ligands docked in both proteins are summarized in supplementary information, SI Tables 1 and 2.

### 4.2. Synthesis of tyramine derivatives

4.2.1. Materials and methods

All the reactions were performed under an atmosphere of argon with oven-dried glassware. Materials and reagents were obtained from commercial suppliers and used without further purification except when otherwise noted. All reaction solutions were magnetically stirred with Teflon stir bars, and temperatures were measured externally. Solvents were distilled under an argon atmosphere prior to use. Dichloromethane was dried over P_2O_5 and triethylamine was distilled over CaH_2. Ethanol and methanol used were reagent-grade solvents. The reaction progress

was monitored on precoated silica gel TLC plates. Spots were visualized under 254 nm UV light and/or by dipping the TLC plate into a solution of phosphomolybdic acid staining reagent, followed by heating. Column chromatography was performed with silica gel (230–400 mesh). ^{1}H and ^{13}C NMR spectra were recorded in MeOD on a 500 MHz Bruker (125 MHz) instrument. Chemical shifts (δ) were reported in parts per million (ppm) downfield from tetramethylsilane as the internal standard, and coupling constants are in hertz (Hz). Assignment of proton resonances was confirmed by correlated spectroscopy. IR spectra were recorded with a universal attenuated total reflection sampling accessory (diamond ATR) on an Agilent Cary 630 FT-IR spectrometer.

4.2.1.1. Synthesis of tyramines 8,9, 17-26. *General procedure*: Substituted cinnamic acid derivatives (1 equiv.) were dissolved in 2.5 mL of dimethylformamide (DMF) and trimethylamine (TEA) (3 equiv., 232 μL). The solution was cooled in an ice bath and substituted tyramine derivative (1.25 equiv.) was added followed by the addition of a solution of PyBOP (1.25 equiv., 362 mg) in dichloromethane (DCM) (2.5 mL). The mixture was stirred at 0 °C for 30 min and then at room temperature for 12 h. The solvent was removed under reduced pressure and the resulting mixture was diluted with water (15 mL). The products are extracted with ethyl acetate (2 × 15 mL). The combined organic extracts were washed sequentially with 1N HCl, water, 1M NaHCO₃ and brine, dried over MgSO₄, filtered and evaporated. The residue was purified on a silica gel column (eluent: ethyl acetate: petroleum ether) to obtain compounds **8**, **9**, **17–26** in 57–83% yield.

4.2.1.2. *(E)-3-(3,4-dihydroxyphenyl)-N-(4-hydroxyphenethyl)acrylamide* **8** *(yield 69%)*. IR (cm^{-1}): 3273, 2492 1649, 1595, 1514, 1463, 1362,
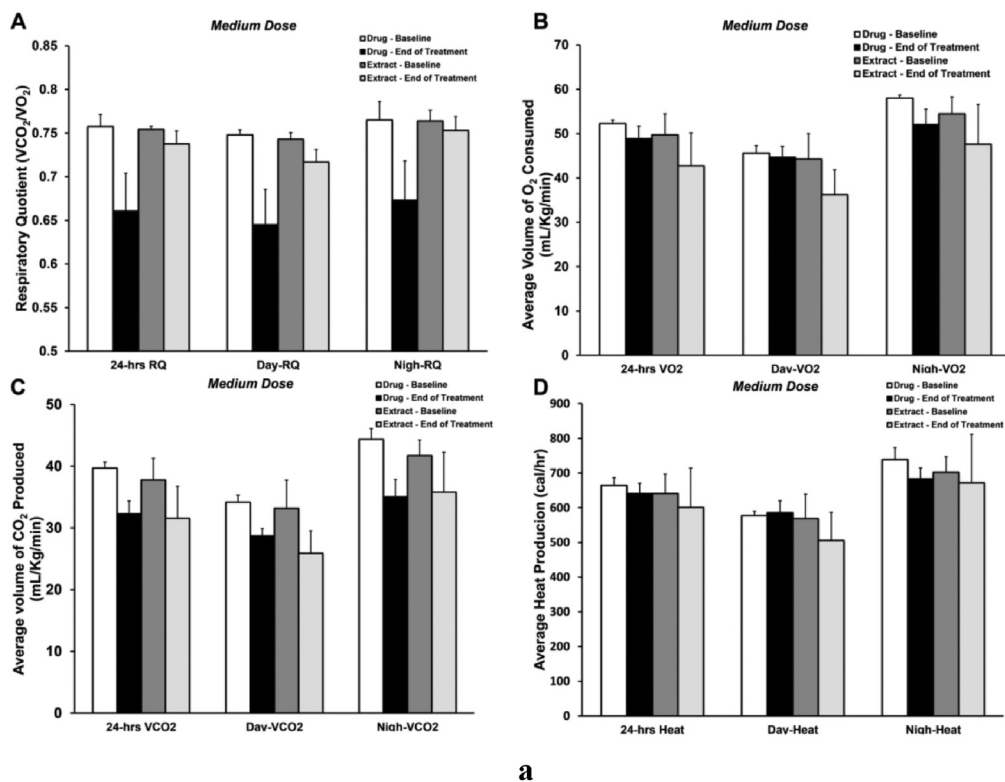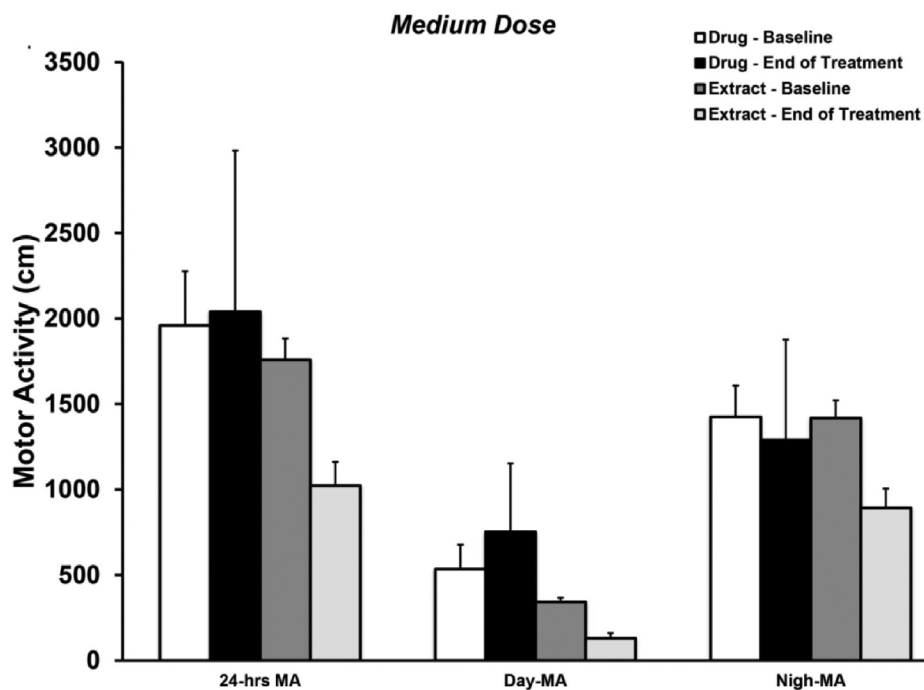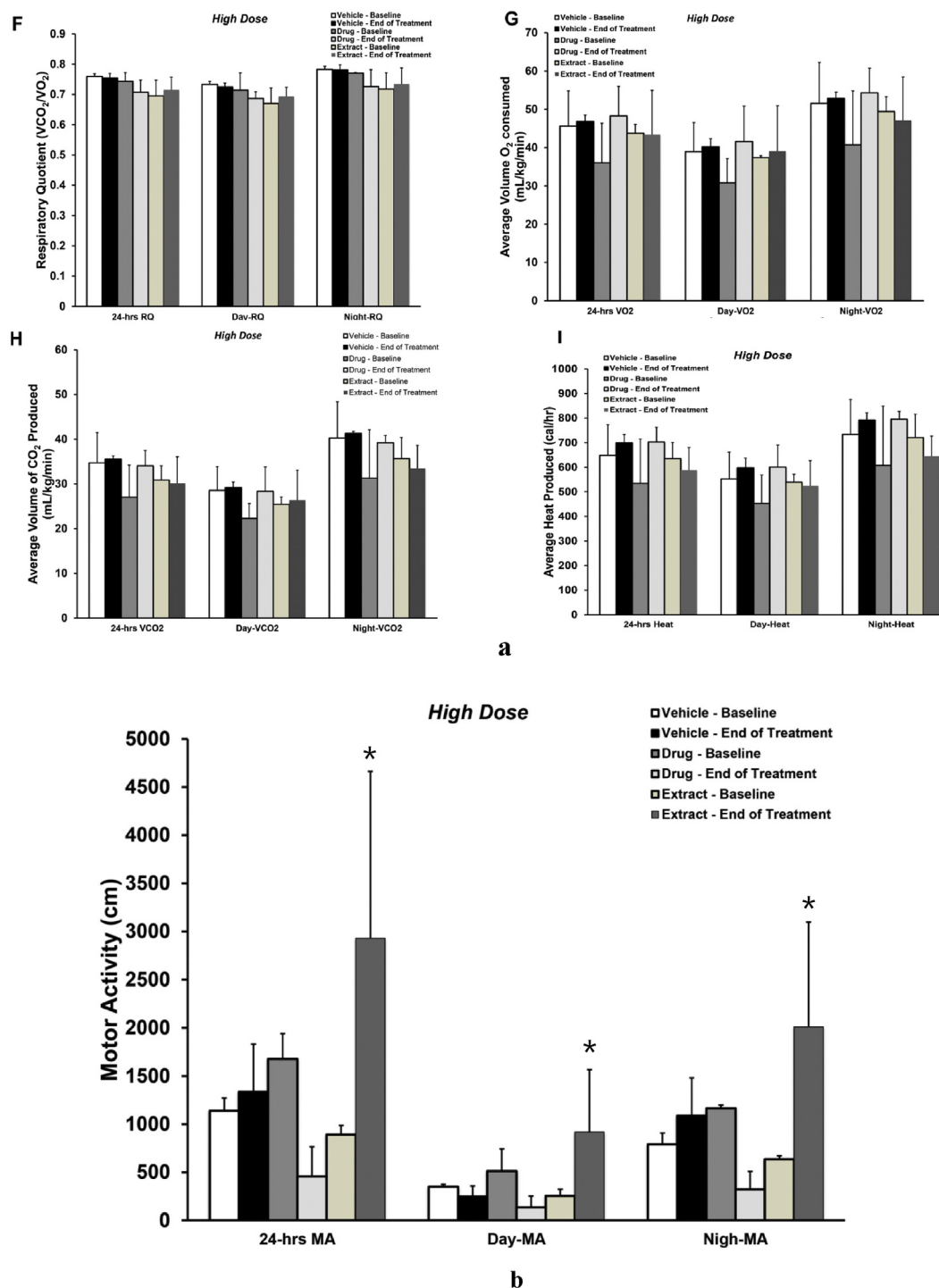
Fig. 7. a. Metabolic data of the medium-dose groups treated with both drug (**9**) and extract (**TEE**): (A) RQ, (B) VO₂, (C) VCO₂, and (D) heat production (Day – Daytime; Nigh – Night time).b. Metabolic data of the medium dose groups treated with both drug (**9**) and extract (**TEE**) (Day-MA – Daytime motor activity; Nigh-MA – Night time motor activity).

a

b

Fig. 8. a. Metabolic data of the high dose groups treated with both **9** and TEE: (F) respiratory quotient, (G) VO_2, (H) VCO_2, and (I) heat.b. Metabolic data of the high dose groups treated with both drug (**9**) and extract (**TEE**) (Day-MA – Daytime motor activity; Nigh-MA – Night time motor activity).

1284, 1242, 1114, 975, 850 and 815; ^{1}H NMR (500 MHz, MeOD) δ 7.41 (d, $J = 15.6$ Hz, 1H), 7.11–7.01 (m, 3H), 6.94–6.88 (m, 1H), 6.79 (d, $J = 8.1$ Hz, 1H), 6.74 (d, $J = 8.4$ Hz, 2H), 6.36 (d, $J = 15.6$ Hz, 1H), 3.52–3.47 (t, $J = 7.3$ Hz, 2H), 2.76(t, $J = 7.3$ Hz, 2H); ^{13}C NMR (125MHz, MeOD) δ 167.9, 155.5, 147.4, 145.3, 140.8, 129.9, 129.4, 126.9, 120.8, 117.0, 115.1, 114.9, 113.7, 41.2, 34.4.

*4.2.1.3. (E)-3-(4-hydroxy-3-methoxyphenyl)-N-(4-hydroxyphenethyl) acrylamide **9** (yield 67%).* IR (cm^{-1}): 3255, 2492, 1651, 1591, 1514, 1459, 1362, 1279, 1126, 1032, 977 and 819; ^{1}H NMR (500 MHz, MeOD)

δ 7.46 (d, $J = 15.6$ Hz, 1H), 7.16–7.01 (m, 5H), 6.81 (d, $J = 8.1$ Hz, 1H), 6.74 (d, $J = 8.4$ Hz, 2H), 6.42 (d, $J = 15.6$ Hz, 1H), 3.88 (s, 3H), 3.54–3.45 (m, 2H), 2.77 (t, $J = 7.3$ Hz, 2H); ^{13}C NMR (125MHz, MeOD) δ 167.8, 155.5, 148.4, 147.9, 140.7, 129.9, 129.4, 126.9, 121.9, 117.4, 115.1, 114.9, 110.1, 55.0, 41.2, 34.4 (Supplementary information, SI Figure C.4 – C.6).

*4.2.1.4. (E)-N-(3,4-dihydroxyphenethyl)-3-(3,4-dihydroxyphenyl)acryl-amide **17** (yield 58%).* IR (cm^{-1}): 3313, 2939, 2487, 2073, 1648, 1579, 1513, 1463, 1439, 1360, 1280, 1203, 1164, 1122, 973, 850 and 811; [1]H
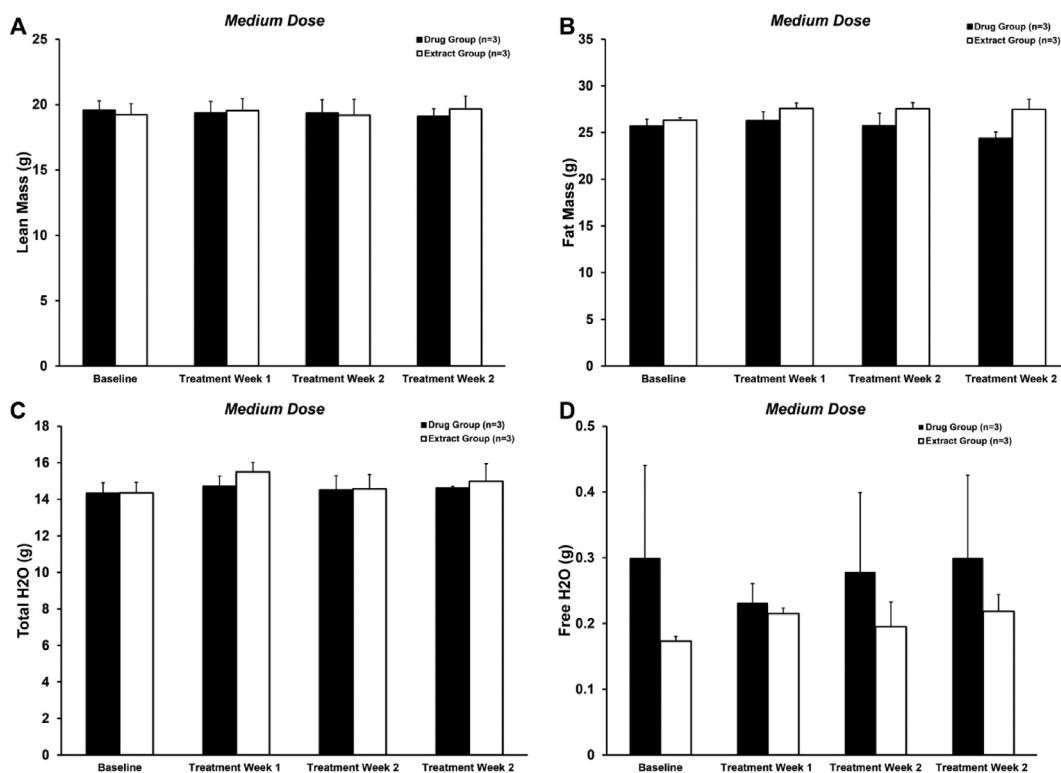
Fig. 9. The body composition of the medium-dose group mice treated with drug **9** and **TEE**: (A) lean mass, (B) fat mass, (C) free water and (D) total water content.
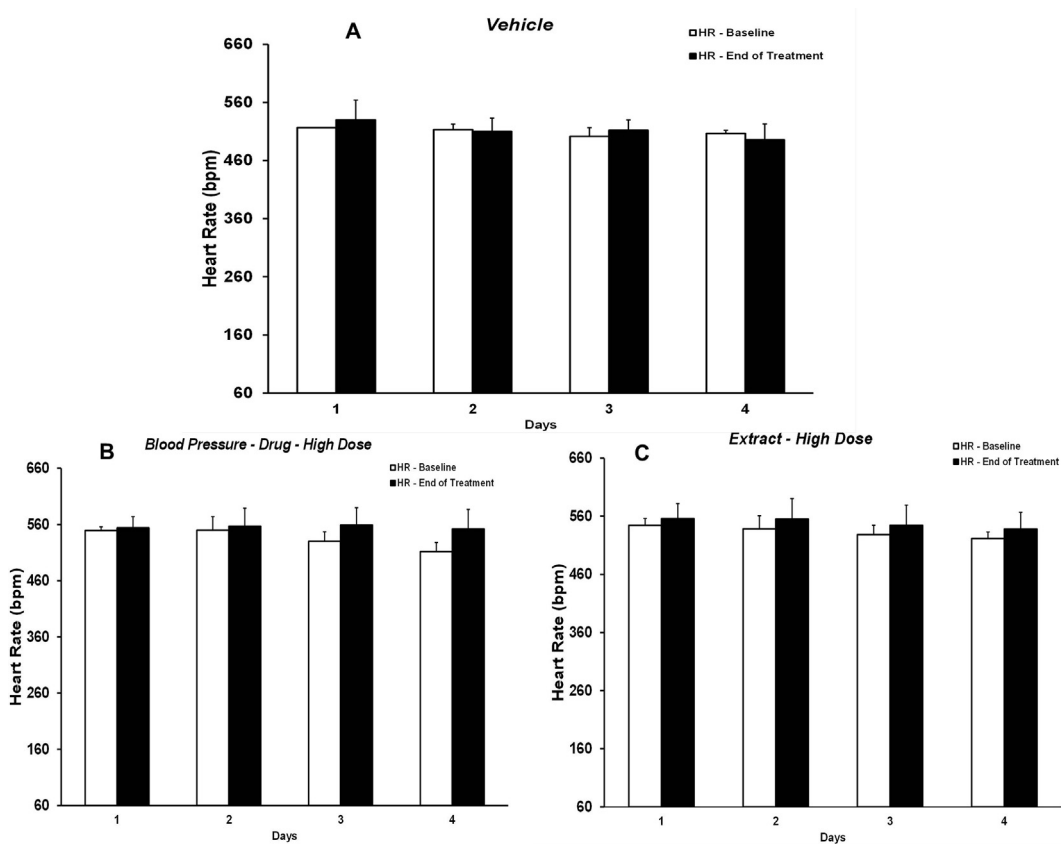

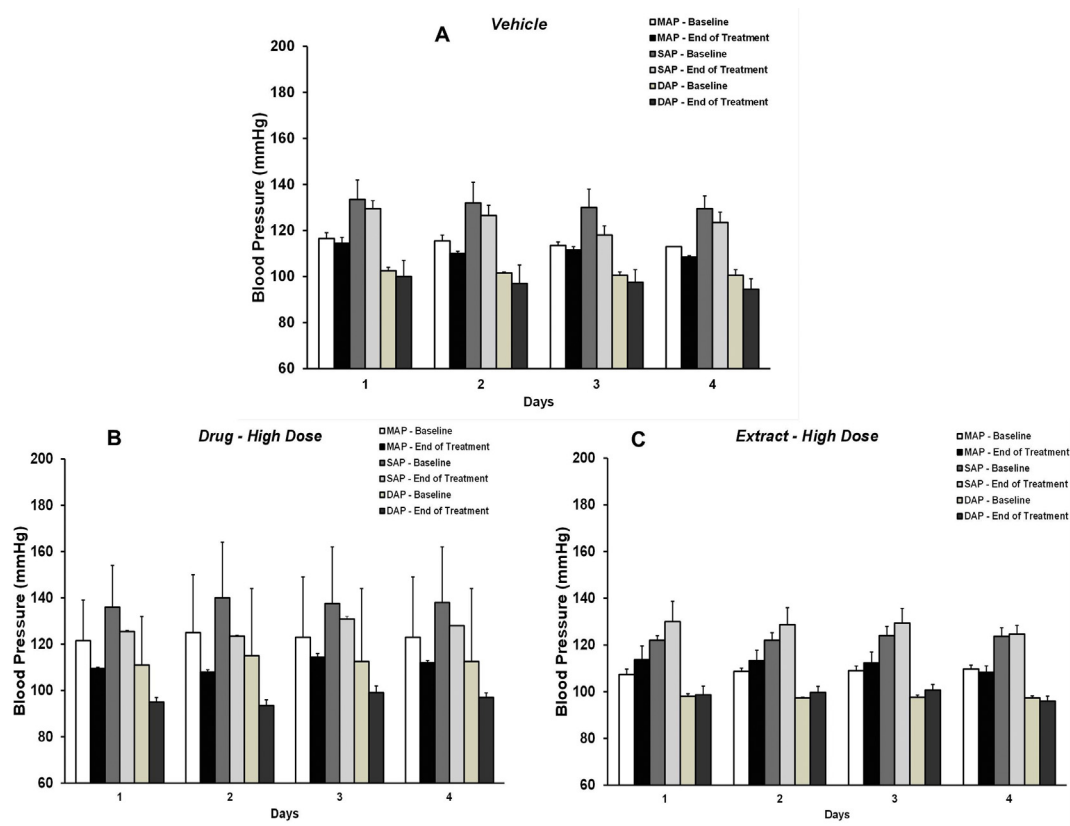**Fig. 10.** Heart rate of high-dose group db/db mice treated with a) vehicle, b) drug **9** and c) extract **TEE**.

Fig. 11. Blood pressure of high-dose group db/db mice treated with a) vehicle b) drug **9** and c) extract **TEE**.

NMR (500 MHz, MeOD) δ 7.40 (d, $J = 15.7$ Hz, 1H), 7.02 (s, 1H), 6.94–6.89 (m, 1H), 6.78 (d, $J = 8.1$ Hz, 1H), 6.73–6.67 (m, 2H), 6.57 (d, $J = 8.0$ Hz, 1H), 6.36 (d, $J = 15.7$ Hz, 1H), 3.46 (t, $J = 7.3$ Hz, 2H), 2.71 (t, $J = 7.3$ Hz, 2H); ^{13}C NMR (125MHz, MeOD) δ 167.9, 147.3, 145.3, 144.9, 143.4, 140.8, 130.7, 126.9, 120.7, 119.7, 117.0, 115.5, 115.0, 113.7, 41.2, 34.7 (Supplementary information, SI Figure C.1 – C.3).

4.2.1.5. (E)-3-(3,4-dihydroxyphenyl)-N-(3-methoxyphenethyl)acrylamide **18** *(yield 65%).* IR (cm^{-1}): 3170, 2944, 2491, 1651, 1585, 1514, 1456, 1362, 1284, 1260, 1203, 1154, 1116, 1039, 978, 851, 814, 783 and 696; ^{1}H NMR (500 MHz, MeOD) δ 7.41 (d, $J = 15.6$ Hz, 1H), 7.19 (t, $J = 8.1$ Hz, 1H), 7.03 (s, 1H), 6.91 (d, $J = 8.1$ Hz, 1H), 6.79 (dt, $J = 12.5, 8.0$ Hz, 5H), 6.36 (d, $J = 15.7$ Hz, 1H), 3.76 (s, 3H), 3.52 (t, $J = 7.3$ Hz, 2H), 2.83 (t, $J = 7.3$ Hz, 2H); ^{13}C NMR (125MHz, MeOD) δ 167.9, 159.9, 147.4, 145.3, 140.9, 140.7, 129.1, 126.9, 120.8, 117.0, 115.1, 113.9, 113.5, 111.5, 54.2, 40.8, 35.3.

4.2.1.6. (E)-N-(3,4-dihydroxyphenethyl)-3-(3-methoxyphenyl)acrylamide **19** *(yield 57%).* IR (cm^{-1}): 3245, 2488, 1655, 1598, 1520, 1489, 1456, 1361, 1280, 1256, 1197, 1116, 1047, 977, 850, 784 and 680;^{1}H NMR (500 MHz, MeOD) δ 7.50 (d, $J = 15.7$ Hz, 1H), 7.29 (t, $J = 7.9$ Hz, 1H), 7.13 (d, $J = 7.6$ Hz, 1H), 7.09 (s, 1H), 6.94 (dd, $J = 8.1, 2.1$ Hz, 1H), 6.71 (dd, $J = 9.7, 4.9$ Hz, 2H), 6.58 (dd, $J = 8.7, 7.0$ Hz, 2H), 3.81 (s, 3H), 3.48 (t, $J = 7.3$ Hz, 2H), 2.72 (t, $J = 7.3$ Hz, 2H); ^{13}C NMR (125MHz, MeOD) δ 167.2, 160.1, 144.9, 143.4, 140.2, 136.3, 130.7, 129.5, 120.8, 120.0, 119.7, 115.5, 115.1, 112.4, 54.3, 41.2, 34.6.

4.2.1.7. (E)-N-(4-hydroxyphenethyl)-3-(3-methoxyphenyl)acrylamide **20** *(yield 83%).* IR (cm^{-1}): 2967, 2868, 2396, 1656, 1610, 1516, 1489, 1453, 1361, 1242, 1206, 1156, 1087, 1048, 1015, 982, 831, 782 and 681; ^{1}H NMR (500 MHz, MeOD) δ 7.50 (d, $J = 15.7$ Hz, 1H), 7.30 (t, $J = 7.9$ Hz, 1H), 7.13 (d, $J = 7.6$ Hz, 1H), 7.11–7.05 (m, 4H), 6.94 (dd, $J = 8.1, 2.0$ Hz, 1H), 6.74 (d, $J = 8.3$ Hz, 2H), 6.59 (d, $J = 15.8$ Hz, 1H), 3.82 (s, 4H), 3.49 (t, $J = 7.4$ Hz, 2H), 2.78 (t, $J = 7.3$ Hz, 2H); ^{13}C NMR (125MHz, MeOD) δ 167.1, 160.1, 155.6, 140.2, 136.3, 129.8, 129.6, 129.4, 120.8, 120.0, 115.1, 114.9, 112.4, 54.4, 41.2, 34.4.

4.2.1.8. (E)-N-(4-hydroxyphenethyl)-3-(3-methoxyphenyl)acrylamide **21** *(yield 82%).* IR (cm^{-1}): 3277, 3070, 2935, 2835, 1655, 1602, 1582, 1546, 1488, 1454, 1433, 1367, 1315, 1209, 1217, 1153, 1039, 979, 849, 779, 695 and 677; ^{1}H NMR (500 MHz, CDCl$_3$) δ 7.60 (d, $J = 15.5$ Hz, 1H), 7.27 (dt, $J = 11.3, 7.8$ Hz, 3H), 7.09 (d, $J = 7.6$ Hz, 1H), 7.02 (s, 1H), 6.91 (d, $J = 8.1$ Hz, 1H), 6.82 (dd, $J = 14.7, 9.4$ Hz, 3H), 6.35 (d, $J = 15.6$ Hz, 1H), 5.83 (bs, 1H), 3.83 (s, 3H), 3.81 (s, 3H), 3.68 (m, 2H), 2.89 (t, $J = 6.8$ Hz, 2H); ^{13}C NMR (125MHz, CDCl$_3$) δ 165.9, 159.9, 140.9, 140.5, 136.2, 129.8, 121.06, 120.4, 115.4, 114.5, 112.9, 111.9, 55.3, 40.7, 35.7.

4.2.1.9. (E)-N-(3,4-dihydroxyphenethyl)-3-(4-hydroxy-3-methoxyphenyl) acrylamide **22** *(yield 65%).* IR (cm^{-1}): 3322, 2492, 1651, 1591, 1515, 1461, 1362, 1280, 1205, 1123, 1032, 976, 845 and 815; ^{1}H NMR (500 MHz, MeOD) δ 7.46 (d, $J = 15.7$ Hz, 1H), 7.12 (s, 1H), 7.03 (dd, $J = 8.1, 1.4$ Hz, 1H), 6.81 (d, $J = 8.1$ Hz, 1H), 6.71 (dd, $J = 9.4, 4.8$ Hz, 2H), 6.57 (dd, $J = 7.8, 1.5$ Hz, 1H), 6.43 (d, $J = 15.7$ Hz, 1H), 3.89 (s, 3H), 3.48 (t, $J = 7.3$ Hz, 2H), 2.72 (t, $J = 7.2$ Hz, 2H); ^{13}C NMR (125MHz, MeOD) δ 167.8, 148.4, 147.9, 144.9, 143.4, 140.6, 130.7, 126.9, 121.8, 119.7, 117.4, 115.5, 115.1, 110.1, 55.0, 41.2, 34.7.

4.2.1.10. (E)-3-(4-hydroxy-3-methoxyphenyl)-N-(3-methoxyphenethyl) acrylamide **23** *(yield 75%).* IR (cm^{-1}): 2938, 2482, 1652, 1600, 1585, 1514, 1456, 1434, 1362, 1281, 1262, 1281, 1262, 1206, 1157, 1125, 1035, 979, 846, 818, 782 and 696; ^{1}H NMR (500 MHz, MeOD) δ 7.46 (d, $J = 15.7$ Hz, 1H), 7.21 (t, $J = 8.0$ Hz, 1H), 7.12 (s, 1H), 7.04 (dd, $J = 8.1, 1.3$ Hz, 1H), 6.82 (t, $J = 7.8$ Hz, 2H), 6.80–6.75 (m, 1H), 6.42 (d, $J = 15.6$ Hz, 1H), 3.89 (s, 3H), 3.78 (s, 3H), 3.54 (t, $J = 7.3$ Hz, 2H), 2.85 (t, $J =$

7.2 Hz, 2H); ^{13}C NMR (125MHz, MeOD) δ 167.8, 159.9, 148.5, 147.9, 140.7, 129.1, 126.8, 121.8, 120.7, 117.3, 115.1, 114.0, 111.5, 110.1, 55.0, 54.2, 40.8, 35.3.

4.2.1.11. (E)-N-(3,4-dihydroxyphenethyl)-3-(4-hydroxy-3,5-dimethoxyphenyl)acrylamide 24 (yield 71%). IR (cm^{-1}): 3339, 2939, 2492, 2071, 1652, 1603, 1514, 1457, 1427, 1337, 1282, 1216, 1156, 1114, 975, 869 and 827; ^{1}H NMR (500 MHz, MeOD) δ 7.43 (d, $J = 15.6$ Hz, 1H), 6.82 (s, 2H), 6.75–6.69 (m, 2H), 6.57 (d, $J = 7.9$ Hz, 1H), 6.45 (d, $J = 15.6$ Hz, 1H), 3.85 (s, 7H), 3.50 (t, $J = 7.2$ Hz, 2H), 2.72 (t, $J = 7.2$ Hz, 2H); ^{13}C NMR (125MHz, MeOD) δ 167.7, 148.0, 144.9, 143.4, 140.9, 137.4, 130.7, 125.9, 119.8, 117.9, 115.6, 115.1, 105.0, 55.4, 41.2, 34.6 (Supplementary information, SI Figure C.7 – C.9).

4.2.1.12. (E)-3-(4-hydroxy-3,5-dimethoxyphenyl)-N-(4-hydroxyphenethyl) acrylamide 25 (yield 69%). IR (cm^{-1}): 3339, 2939, 2493, 2071, 1652, 1603, 1514, 1457, 1427, 1337, 1282, 1216, 1156, 1114, 975, 868 and 827; ^{1}H NMR (500 MHz, MeOD) δ 7.44 (d, $J = 15.6$ Hz, 1H), 7.06 (d, $J = 8.2$ Hz, 2H), 6.83 (s, 2H), 6.74 (d, $J = 8.2$ Hz, 2H), 6.45 (d, $J = 15.6$ Hz, 1H), 3.86 (s, 6H), 3.49 (t, $J = 7.3$ Hz, 2H), 2.77 (t, $J = 7.2$ Hz, 2H); ^{13}C NMR (125MHz, MeOD) δ 167.7, 155.57, 148.0, 140.9, 137.5, 129.9, 129.4, 125.8, 117.8, 114.9, 105.0, 55.4, 41.2, 34.4.

4.2.1.13. (E)-3-(4-hydroxy-3,5-dimethoxyphenyl)-N-(3-methoxyphenethyl)acrylamide 26 (yield 72%). IR (cm^{-1}): 3282, 2938, 2839, 2252, 1655, 1602, 1513, 1490, 1455, 1425, 1320, 1285, 1259, 1209, 1153, 1112, 1061, 1038, 976, 907, 828, 780 and 696; ^{1}H NMR (500 MHz, MeOH) δ 7.52 (d, $J = 15.5$ Hz, 1H), 7.22 (t, $J = 7.9$ Hz, 1H), 6.79 (dd, $J = 16.6, 6.9$ Hz, 3H), 6.70 (s, 2H), 6.27 (d, $J = 15.5$ Hz, 1H), 6.09 (s, 1H), 6.02 (s, 1H), 3.84 (s, 6H), 3.77 (s, 3H), 3.69–3.61 (m, 2H), 2.86 (t, $J = 6.7$ Hz, 2H); ^{13}C NMR (125MHz, MeOH) δ 166.2, 159.8, 147.2, 141.1, 140.6, 136.6, 129.6, 126.3, 121.1, 118.7, 114.5, 111.8, 104.8, 56.3, 55.2, 40.7, 35.7.

4.2.2. Synthesis of compounds 6, 27–37

General Procedure: The unsaturated tyramine derivatives (**8, 9, 17–26**) (0.150 mmol) were dissolved in methanol (1.5 mL) and to this solution, palladium on carbon 5% (0.010 g, 0.0944 mmol) was added and purged with hydrogen gas. The resulting mixture was stirred for 12 h at room temperature under hydrogen atmosphere (with H$_2$ filled balloon). After 12 h, the reaction mixture was filtered over Celite, washed with methanol (2 × 10 mL) and the combined washings were concentrated and purified by flash column chromatography using chloroform and methanol (94:6) to yield the saturated amide derivatives (**6, 27–37**) in 49–90% yield.

4.2.2.1. 3-(3,4-Dihydroxyphenyl)-N-(4-hydroxyphenethyl)propanamide 6 (yield 68%). IR (cm^{-1}): 3282, 2499, 1610, 1515, 1449, 1361, 1284, 1242, 1115, 976 and 819; ^{1}H NMR (500 MHz, MeOD) δ 6.97 (d, $J = 8.3$ Hz, 2H), 6.69 (dd, $J = 20.7, 11.9$ Hz, 4H), 6.53 (d, $J = 6.5$ Hz, 1H), 3.32 (dd, $J = 12.7, 5.1$ Hz, 2H), 2.75 (t, $J = 7.5$ Hz, 2H), 2.63 (t, $J = 7.3$ Hz, 2H), 2.39 (t, $J = 7.6$ Hz, 2H); ^{13}C NMR (125MHz, MeOD) δ 174.0, 155.4, 144.8, 132.4, 129.9, 129.3, 119.2, 115.2, 115.0, 114.8, 40.9, 38.0, 34.3, 31.1.

4.2.2.2. N-(3,4-dihydroxyphenethyl)-3-(3,4-dihydroxyphenyl)propanamide 27 (yield 49%). IR (cm^{-1}):3314, 2935, 2501, 2073, 1599, 1517, 1481, 1440, 1359, 1282, 1199, 1152, 1115, 972, 870, 811 and 783; ^{1}H NMR (500 MHz, MeOD) δ 6.69 (dd, $J = 8.0, 1.2$ Hz, 2H), 6.65 (dd, $J = 5.7, 1.6$ Hz, 2H), 6.52 (dd, $J = 8.0, 1.6$ Hz, 1H), 6.48 (dd, $J = 7.9, 1.6$ Hz, 1H), 3.33–3.27 (m, 2H), 2.75 (t, $J = 7.6$ Hz, 2H), 2.57 (t, $J = 7.7$ Hz, 2H), 2.39 (t, $J = 7.7$ Hz, 2H); ^{13}C NMR (125MHz, MeOD) δ 174.1, 144.8, 143.3, 132.4, 130.7, 119.7, 119.2, 115.5, 115.2, 114.9, 114.9, 40.9, 38.1, 34.6, 31.1.

4.2.2.3. 3-(3,4-dihydroxyphenyl)-N-(3-methoxyphenethyl)propanamide 28 (yield 62%). IR (cm^{-1}): 3276, 2938, 2491, 1595, 1515, 1453, 1437, 1360, 1282, 1201, 1166, 1152, 1116, 1061, 1038, 869, 812, 781, 743 and 696; ^{1}H NMR (500 MHz, MeOD) δ 7.18 (t, $J = 8.0$ Hz, 1H), 6.71 (ddd, $J = 21.9, 13.9, 4.1$ Hz, 5H), 6.55–6.48 (m, 1H), 3.76 (s, 3H), 3.40–3.32 (m, 3H), 2.72 (dt, $J = 20.7, 7.3$ Hz, 4H), 2.39 (t, $J = 7.6$ Hz, 2H); ^{13}C NMR (125MHz, MeOD) δ 174.1, 159.9, 144.8, 143.2, 140.7, 132.4, 129.1, 120.8, 119.2, 115.2, 114.9, 113.9, 111.5, 54.2, 40.5, 38.1, 35.2, 31.1.

4.2.2.4. N-(3,4-dihydroxyphenethyl)-3-(3-methoxyphenyl)propanamide 29 (yield 69%). IR (cm^{-1}): 3280, 2939,2507, 1627, 1602, 1519, 1485, 1465, 1455, 1440, 1359, 1278, 1260, 1197, 1152, 1116, 1049, 872, 784 and 697; ^{1}H NMR (500 MHz, MeOD) δ 7.18 (t, $J = 8.0$ Hz, 1H), 6.81–6.73 (m, 3H), 6.69 (d, $J = 8.0$ Hz, 1H), 6.64 (d, $J = 1.4$ Hz, 1H), 6.47 (d, $J = 6.4$ Hz, 1H), 3.78 (s, 3H), 3.32 (t, $J = 7.6$ Hz, 2H), 2.87 (t, $J = 7.6$ Hz, 2H), 2.58 (t, $J = 7.3$ Hz, 2H), 2.45 (t, $J = 7.3$ Hz, 2H); ^{13}C NMR (125MHz, MeOD) δ 173.8, 159.9, 144.9, 143.4, 142.4, 130.7, 129.0, 120.3, 119.7, 115.4, 114.9, 113.7, 111.3, 54.2, 40.9, 37.5, 34.5, 31.6.

4.2.2.5. N-(4-hydroxyphenethyl)-3-(3-methoxyphenyl)propanamide 30 (yield 91%). IR (cm^{-1}): 2947, 2868, 1635, 1614, 1516, 1455, 1362, 1261, 1261, 1207, 1153, 1087, 1015, 831, 780 and 697; ^{1}H NMR (500 MHz, MeOD) δ 7.18 (t, $J = 8.0$ Hz, 1H), 6.96 (d, $J = 8.3$ Hz, 2H), 6.82–6.74 (m, 3H), 6.71 (d, $J = 8.4$ Hz, 2H), 3.77 (s, 3H), 3.35–3.29 (m, 2H), 2.87 (t, $J = 7.6$ Hz, 2H), 2.62 (t, $J = 7.6$ Hz, 2H), 2.45 (t, $J = 7.6$ Hz, 2H); ^{13}C NMR (125MHz, MeOD) δ 173.7, 159.9, 155.5, 142.4, 129.9, 129.3, 129.1, 120.4, 114.9, 113.7, 111.3, 54.2, 40.9, 37.5, 34.3, 31.6.

4.2.2.6. N-(3-methoxyphenethyl)-3-(3-methoxyphenyl)propanamide 31 (yield 77%). IR (cm^{-1}): 3294, 2937, 1644, 1602, 1585, 1547, 1490, 1455, 1260, 1152, 1041, 874, 780 and 696; ^{1}H NMR (500 MHz, MeOD) δ 7.18 (dd, $J = 10.6, 5.4$ Hz, 2H), 6.82–6.72 (m, 6H), 3.78 (s, 6H), 3.40–3.35 (m, 2H), 2.87 (t, $J = 7.7$ Hz, 2H), 2.71 (t, $J = 7.3$ Hz, 2H), 2.46–2.42 (t, $J = 7.3$ Hz, 2H); ^{13}C NMR (125MHz, MeOD) δ 173.8, 159.9, 142.3, 140.6, 129.0, 120.7, 120.3, 113.9, 113.8, 111.4, 111.2, 54.2, 40.5, 37.5, 35.2, 31.6.

4.2.2.7. N-(3,4-dihydroxyphenethyl)-3-(4-hydroxy-3-methoxyphenyl)propanamide 32 (yield 59%). IR (cm^{-1}): 3338, 2938, 2500, 1600, 1516, 1465, 1449, 1362, 1275, 1153, 1123, 1034, 976, 870 and 814; ^{1}H NMR (500 MHz, MeOD) δ 6.78 (d, $J = 1.7$ Hz, 1H), 6.72 (d, $J = 8.0$ Hz, 1H), 6.69 (d, $J = 8.0$ Hz, 1H), 6.63 (dd, $J = 5.8, 1.9$ Hz, 2H), 6.46 (dd, $J = 8.0, 1.9$ Hz, 1H), 3.83 (s, 3H), 3.30 (d, $J = 7.6$ Hz, 2H), 2.81 (t, $J = 7.6$ Hz, 2H), 2.58 (t, $J = 7.7$ Hz, 2H), 2.42 (t, $J = 7.7$ Hz, 2H); ^{13}C NMR (125MHz, MeOD) δ 174.1, 147.5, 144.9, 144.5, 143.4, 132.4, 130.7, 120.4, 119.7, 115.4, 114.9, 114.8, 111.7, 54.9, 40.9, 38.0, 34.6, 31.3.

4.2.2.8. 3-(4-Hydroxy-3-methoxyphenyl)-N-(4-hydroxyphenethyl)propanamide 33 (yield 88%). IR (cm^{-1}): 3279, 2938, 2499, 1627, 1613, 1596, 1515, 1465, 1452, 1436, 1363, 1236, 1153, 1125, 1034 and 822; ^{1}H NMR (500 MHz, MeOD) δ 6.95 (d, $J = 8.4$ Hz, 2H), 6.78 (d, $J = 1.7$ Hz, 1H), 6.74–6.69 (m, 3H), 6.64 (dd, $J = 8.0, 1.7$ Hz, 1H), 3.84 (s, 3H), 3.33–3.28 (m, 2H), 2.81 (t, $J = 7.5$ Hz, 2H), 2.62 (t, $J = 7.3$ Hz, 2H), 2.42 (t, $J = 7.5$ Hz, 2H); ^{13}C NMR (125MHz, MeOD) δ 173.97, 155.47, 147.48, 144.50, 132.33, 129.88, 129.3, 120.4, 114.8, 114.8, 111.8, 54.9, 40.9, 37.9, 34.3, 31.2.

4.2.2.9. 3-(4-Hydroxy-3-methoxyphenyl)-N-(3-methoxyphenethyl)propanamide 34 (yield 90%). IR (cm^{-1}): 2937, 2488, 1631, 1600, 1516, 1465, 1433, 1363, 1260, 1153, 1125, 1037, 854, 787 and 697; ^{1}H NMR (500 MHz, MeOD) δ 7.17 (dd, $J = 8.8, 7.6$ Hz, 1H), 6.81–6.74 (m, 3H), 6.72 (d, $J = 7.9$ Hz, 2H), 6.63 (dd, $J = 8.0, 1.8$ Hz, 1H), 3.83 (s, 4H), 3.78 (d, $J = 7.9$ Hz, 3H), 3.37 (t, $J = 7.3$ Hz, 2H), 2.81 (t, $J = 7.6$ Hz, 2H), 2.70

(t, *J* = 7.3 Hz, 2H), 2.42 (t, *J* = 7.6 Hz, 2H); ^{13}C NMR (125MHz, MeOD) δ 174.0, 159.9, 147.5, 144.5, 140.6, 132.3, 129.1, 120.7, 120.4, 114.8, 113.9, 111.7, 111.4, 54.9, 54.2, 40.5, 37.9, 35.2, 31.2.

4.2.2.10. N-(3,4-dihydroxyphenethyl)-3-(4-hydroxy-3,5-dimethoxyphenyl) propanamide 35 (yield 87%). IR (cm^{-1}): 3348, 2939, 2499, 1611, 1519, 1461, 1345, 1282, 1215, 1114, 977 and 814; ^{1}H NMR (500 MHz, MeOD) δ 6.68 (d, *J* = 8.0 Hz, 1H), 6.63 (d, *J* = 1.9 Hz, 1H), 6.52–6.47 (m, 2H), 6.45 (dd, *J* = 8.0, 1.9 Hz, 1H), 3.82 (s, 6H), 3.33–3.29 (m, 2H), 2.82 (t, *J* = 7.5 Hz, 2H), 2.75 (t, *J* = 7.6 Hz, 2H), 2.43 (t, *J* = 7.6 Hz, 2H); ^{13}C NMR (125MHz, MeOD) δ 173.9, 147.8, 144.9, 143.3, 133.5, 131.6, 130.6, 119.7, 115.4, 114.9, 105.3, 55.3, 40.9, 37.9, 34.6, 31.7.

4.2.2.11. 3-(4-Hydroxy-3,5-dimethoxyphenyl)-N-(4-hydroxyphenethyl) propanamide 36 (yield 90%). IR (cm^{-1}): 2941, 2506, 2189, 2028, 1621, 1603, 1512, 1486, 1456, 1437, 1351, 1328, 1260, 1242, 1139, 1050, 969, 837 and 757; ^{1}H NMR (500 MHz, MeOD) δ 6.94 (d, *J* = 8.4 Hz, 2H), 6.70 (d, *J* = 8.4 Hz, 2H), 6.48 (s, 2H), 3.83 (s, 7H), 3.36–3.30 (m, 4H), 2.82 (t, *J* = 7.5 Hz, 2H), 2.62 (t, *J* = 7.3 Hz, 2H), 2.43 (t, *J* = 7.5 Hz, 2H); ^{13}C NMR (125MHz, MeOD) δ 173.9, 155.4, 147.8, 133.5, 131.6, 129.9, 129.4, 114.9, 105.3, 55.5, 40.9, 38.1, 34.4, 31.8.

4.2.2.12. 3-(4-Hydroxy-3,5-dimethoxyphenyl)-N-(3-methoxyphenethyl) propanamide 37 (yield 89%). IR (cm^{-1}): 3299, 2938, 2838, 2496, 1633, 1603, 1518, 1458, 1429, 1326, 1259, 1213, 1152, 1114, 1040, 908, 830, 785 and 697; ^{1}H NMR (500 MHz, MeOD) δ 7.21–7.14 (m, 1H), 6.75 (d, *J* = 6.0 Hz, 2H), 6.70 (d, *J* = 7.5 Hz, 1H), 6.49 (s, 2H), 3.82 (s, 7H), 3.77 (s, 3H), 3.37 (t, *J* = 7.3 Hz, 2H), 2.82 (t, *J* = 7.5 Hz, 2H), 2.70 (t, *J* = 7.3 Hz, 2H), 2.43 (t, *J* = 7.5 Hz, 2H); ^{13}C NMR (125MHz, MeOD) δ 173.9, 159.9, 147.8, 140.6, 133.6, 131.6, 129.1, 120.7, 113.9, 111.4, 105.3, 55.3, 54.2, 40.5, 37.9, 35.2, 31.7.

4.3. Preparation of the tyramine-enriched extract (TEE) of L. chinense

The root bark of *L. chinense* (2 kg) was extracted with methanol (8 L) at room temperature to get the crude extract (345.5 g). This methanolic extract was suspended in water and successively partitioned between hexanes and ethyl acetate and 35.1 grams of crude material was obtained from the ethyl acetate extract. The crude material (33 g) was dissolved in ethyl acetate (300 mL) and washed with 5% HCl in water (approx. 1 L) and the aqueous layer was further extracted with ethylactate (2 × 300 mL) to yield crude material (20.6 g). This ethyl acetate fraction (18.0 g) was subjected to Sephadex LH-20 column chromatography with CHCl₃:MeOH (1:1) as a solvent to get three fractions (1–3), LC-MS analysis indicated tyramine compounds are in fraction 3 (6.49 g) which was further chromatographed over Sephadex LH-20 column chromatography with MeOH to get three sub-fractions. Analysis of the third sub-fraction by comparative TLC using a pure tyramine **9** indicated that it is a tyramine enriched fraction, **TEE**. The calculated concentration of the tyramines in TEE is 21% based on the reported isolation yields [37].

4.4. In vitro testing

Ciprofibrate and rosiglitazone **1**, were obtained from Cayman Chemical (Ann Arbor, MI). Dulbecco's Modified Eagle's Medium (DMEM), fetal bovine serum (FBS) and phosphate-buffered saline (PBS) were purchased from Hyclone (South Logan, Utah). Penicillin/streptomycin and trypsin were procured from Gibco (Grand Island, NY). Specific plasmids pSG5–PPARα (plasmid 22751) and PPRE X3-tk-luc (plasmid 1015) were obtained from Addgene (Cambridge, MA). pCMV-rPPARγ and pPPREaP2-tk-luc were provided by Dr. Dennis Feller (Department of Pharmacology, University of Mississippi).

4.4.1. Reporter gene assay for the activation of PPARs

Cell-based reporter gene assay for the identification of PPARα and PPARγ agonists was carried out in human hepatoma (HepG2) cells as described previously [41, 44]. Briefly, HepG2 cells were cultured in Dulbecco's Modified Eagle's Medium (DMEM), supplemented with 10% fetal bovine serum (FBS), 100 units/mL penicillin, and 100 μg/mL streptomycin in a humidified atmosphere of 5% CO₂ at 37 °C. HepG2 cells were transfected with either pSG5-PPARα and PRE X3-tk-luc or pCMV-rPPARγ and pPPREaP2-tk-luc plasmid DNA (25 μg of each/1.5 mL cell suspension) by electroporation at 160 V for a single 70 ms pulse using a BTX Electro Square Porator T820 (BTX, San Diego, CA). Transfected cells were plated at a density of 5 × 10^{4} cells/well in 96-well tissue culture plates and grown for 24 h. The cells were treated with various concentrations of the test samples, ciprofibrate or rosiglitazone **1** (30 μM). After incubation for 24 h, the cells were lysed and the luciferase activity was measured using a luciferase assay system (Promega, Madison, WI). The fold activation of luciferase activity in sample-treated cells was calculated in comparison to the vehicle-treated cells.

4.5. In vivo testing

The experimental procedures and protocols for these studies followed the National Institutes of Health *Guide for the Care and Use of Laboratory Animals* and were approved by the Institutional Animal Care and Use Committee of the University of Mississippi Medical Center.

4.5.1. Animals

Male diabetic db/db mice from the Jackson Laboratories (Ann Arbor, MI, USA) at 12 weeks of age were used in these studies. The mice were divided into medium- (n = 6) and high-dose groups (n = 8). In the medium-dose group, mice were treated with 16 mg/kg of **TEE** (n = 3) or 8 mg/kg of **9**. In the high-dose group (n = 8), mice were treated with vehicle (n = 3), 32 mg/kg of **9** (n = 3, out of which 1 mouse died during treatment) or 64 mg/kg of extract **TEE**. The animals were followed for one to two weeks control period before treatment was started. In the medium-dose groups, EchoMRIs were performed during control and experimental periods. High-dose group mice were implanted with transmitters to record the blood pressure and heart rate 24-hr/day for 3 consecutive days. Animals were dosed by gavage.

4.5.2. Body weight and body composition analysis

Male db/db mice were individually housed and fed standard chow (Harlan Teklad, WI). Body weight and food intakes were measured weekly, starting at 12 weeks through 16 weeks of age in order to examine the role of *Lycium Chinense* in regulating body weight. Body composition measurements were performed using magnetic resonance imaging (EchoMRI-900TM, Echo Medical System, Houston, TX) to quantify lean mass, fat mass, and free water and total water content in conscious mice.

4.5.3. Glucose tolerance test

D-glucose (3 mg/g of lean tissue plus 1 mg/g of fat mass) was administered by gavage after a 6-hour fast in 12, 14 and 15-week-old male db/db mice (n = 9). Blood samples were collected by tail snip and blood glucose was measured at 0, 15, 30, 60, 90 and 120 min after glucose injection using glucose strips (ReliOn™).

4.5.4. Telemetry probe implantation

Male db/db mice were anesthetized with 2% isoflurane and, under sterile conditions, a telemetry probe (TA11PA-C10, Data Science, MN) was implanted in the left carotid artery for determination of mean arterial pressure (MAP) and heart rate (HR) 24 hours per day using computerized methods for data collection as previously described [45, 46]. MAP and HR were obtained from the average of 24 h of recording

using a sampling rate of 1000 Hz with a duration of 10 s every 10-minute period.

4.5.5. Experimental design for Telemetry probe implantation

4.5.5.1. Chronic **9** and TEE (Lycium Chinense) treatment.
After 6–16 days of baseline measurements, the mice were randomly assigned to one of three groups and maintained for the remaining 18 days of the study: **TEE** (n = 3), mice were dosed by daily oral gavage (0.3 ml); 2) drug treated-high dose (n = 3), mice were dosed by daily 32 mg/kg; and 3) drug treated-medium-dose (n = 3), mice were dosed by daily 8 mg/kg. After an 8–10 day post-surgery recovery period and 5 days of stable baseline control measurements, **TEE** or drug was given at the high-dose by gavage for 18 days. MAP and HR were recorded daily. In addition, the glucose tolerance test was performed during baseline control and repeated at the end of one and two weeks of treatment.

4.5.5.2. Oxygen consumption and motor activity.
In separate experiments, db/db mice were placed individually in metabolic cages (AccuScan Instruments Inc, Columbus, OH) equipped with oxygen sensors to measure oxygen consumption (VO_2) and infrared beams to determine motor activity. VO_2 was measured for 2 min at 10-minute intervals continuously, 24-hours a day using a Zirconia oxygen sensor. Motor activity in X, Y and Z axes was determined using infrared light beams mounted in the cages. After the mice were acclimatized to the new environment for approximately 4–6 days, VO_2 and animal activity were recorded for 3 consecutive days. Then the mice were administered by gavage, TEE, high- and medium-doses of *L. Chinense* for 18 days and then placed in metabolic cages during the last 4 days of treatment.

Declarations

Author contribution statement

Amar G Chittiboyina, Chinni Yalamanchili, Saqlain Haider: Conceived and designed the experiments.

Yelkaira Vasquez, Shabana Khan, Jussara M do Carmo, Alexandre A. da Silva, Mark Pinkerton John E Hall: Performed the experiments.

Larry A. Walker, Ikhlas A. Khan: Contributed reagents, materials, analysis tools or data.

Competing interest statement

The authors declare no conflict of interest.

Additional information

Supplementary content related to this article has been published online at https://doi.org/10.1016/j.heliyon.2019.e02782.

References

[1] Z. Tao, A. Shi, J. Zhao, Epidemiological perspectives of diabetes, Cell Biochem. Biophys. 73 (2015) 181–185.
[2] A.D. Association. http://www.diabetes.org/diabetes-basics/statistics/?loc=db-slab nav, 2016.
[3] A.R. Vasudevan, A. Balasubramanyam, Thiazolidinediones: a review of their mechanisms of insulin sensitization, therapeutic potential, clinical efficacy, and tolerability, Diabetes Technol. Ther. 6 (2004) 850–863.
[4] R.T. Nolte, G.B. Wisely, S. Westin, J.E. Cobb, M.H. Lambert, R. Kurokawa, M.G. Rosenfeld, T.M. Willson, C.K. Glass, M.V. Milburn, Ligand binding and co-activator assembly of the peroxisome proliferator-activated receptor-γ, Nature 395 (1998) 137–143.
[5] C.V. Rizos, M. Elisaf, D.P. Mikhailidis, E.N. Liberopoulos, How safe is the use of thiazolidinediones in clinical practice? Expert Opin. Drug Saf. 8 (2009) 15–32.
[6] A. Elbrecht, Y. Chen, A. Adams, J. Berger, P. Griffin, T. Klatt, B. Zhang, J. Menke, G. Zhou, R.G. Smith, L-764406 is a partial agonist of human peroxisome proliferator-activated receptor gamma. The role of Cys313 in ligand binding, J. Biol. Chem. 274 (1999) 7913–7922.
[7] F.M. Gregoire, F. Zhang, H.J. Clarke, T.A. Gustafson, D.D. Sears, S. Favelyukis, J. Lenhard, D. Rentzeperis, L.E. Clemens, Y. Mu, MBX-102/JNJ39659100, a novel peroxisome proliferator-activated receptor-ligand with weak transactivation activity retains antidiabetic properties in the absence of weight gain and edema, Mol. Endocrinol. 23 (2009) 975–988.
[8] B.Y. Hwang, J.-H. Lee, J.B. Nam, H.S. Kim, Y.S. Hong, J.J. Lee, Two new furanoditerpenes from saururus c hinensis and their effects on the activation of peroxisome proliferator-activated receptor γ, J. Nat. Prod. 65 (2002) 616–617.
[9] U. Kintscher, M. Goebel, INT-131, a PPARgamma agonist for the treatment of type 2 diabetes, Curr. Opin. Investig. Drugs 10 (2009) 381–387.
[10] Y. Li, Z. Wang, N. Furukawa, P. Escaron, J. Weiszmann, G. Lee, M. Lindstrom, J. Liu, X. Liu, H. Xu, T2384, a novel antidiabetic agent with unique peroxisome proliferator-activated receptor γ binding properties, J. Biol. Chem. 283 (2008) 9168–9176.
[11] F. Chang, L.A. Jaber, H.D. Berlie, M.B. O'Connell, Evolution of peroxisome proliferator-activated receptor agonists, Ann. Pharmacother. 41 (2007) 973–983.
[12] A. Furukawa, T. Arita, S. Satoh, K. Wakabayashi, S. Hayashi, Y. Matsui, K. Araki, M. Kuroha, J. Ohsumi, Discovery of a novel selective PPARγ modulator from (−)-Cercosporamide derivatives, Bioorg. Med. Chem. Lett 20 (2010) 2095–2098.
[13] A. Sugawara, A. Uruno, M. Kudo, K. Matsuda, C.W. Yang, S. Ito, Effects of PPARgamma on hypertension, atherosclerosis, and chronic kidney disease, Endocr. J. 57 (2010) 847–852.
[14] A.G. Atanasov, J.N. Wang, S.P. Gu, J. Bu, M.P. Kramer, L. Baumgartner, N. Fakhrudin, A. Ladurner, C. Malainer, A. Vuorinen, Honokiol: a non-adipogenic PPARγ agonist from nature, Biochim. Biophys. Acta Gen. Subj. 1830 (2013) 4813–4819.
[15] W. Lee, J. Ham, H.C. Kwon, Y.K. Kim, S.-N. Kim, Anti-diabetic effect of amorphastilbol through PPARα/γ dual activation in db/db mice, Biochem. Biophys. Res. Commun. 432 (2013) 73–79.
[16] L. Wang, B. Waltenberger, E.-M. Pferschy-Wenzig, M. Blunder, X. Liu, C. Malainer, T. Blazevic, S. Schwaiger, J.M. Rollinger, E.H. Heiss, Natural product agonists of peroxisome proliferator-activated receptor gamma (PPARγ): a review, Biochem. Pharmacol. 92 (2014) 73–89.
[17] C. Weidner, J.C. de Groot, A. Prasad, A. Freiwald, C. Quedenau, M. Kliem, A. Witzke, V. Kodelja, C.-T. Han, S. Giegold, Amorfrutins are potent antidiabetic dietary natural products, Proc. Natl. Acad. Sci. 109 (2012) 7257–7262.
[18] C. Weidner, S.J. Wowro, A. Freiwald, K. Kawamoto, A. Witzke, M. Kliem, K. Siems, L. Müller-Kuhrt, F.C. Schroeder, S. Sauer, Amorfrutin B is an efficient natural peroxisome proliferator-activated receptor gamma (PPARγ) agonist with potent glucose-lowering properties, Diabetologia 56 (2013) 1802–1812.
[19] O. Potterat, Goji (*Lycium barbarum* and L. chinense): phytochemistry, pharmacology and safety in the perspective of traditional uses and recent popularity, Planta Med. 76 (2010) 7–19.
[20] R. Bo, S. Zheng, J. Xing, L. Luo, Y. Niu, Y. Huang, Z. Liu, Y. Hu, J. Liu, Y. Wu, D. Wang, The immunological activity of *Lycium barbarum* polysaccharides liposome in vitro and adjuvanticity against PCV2 in vivo, Int. J. Biol. Macromol. 85 (2016) 294–301.
[21] R.C.-C. Chang, K.-F. So, *Lycium Barbarum* and Human Health, Springer, 2015.
[22] X. Deng, X. Li, S. Luo, Y. Zheng, X. Luo, L. Zhou, Antitumor activity of *Lycium barbarum* polysaccharides with different molecular weights: an in vitro and in vivo study, Food Nutr. Res. 61 (2017) 1399770.
[23] D. Gao, Q. Li, Z. Liu, Y. Li, Z. Liu, Y. Fan, K. Li, Z. Han, J. Li, Hypoglycemic effects and mechanisms of action of Cortex Lycii Radicis on alloxan-induced diabetic mice, J. Pharm. Soc. Jpn. 127 (2007) 1715–1721.
[24] M. Jin, Q. Huang, K. Zhao, P. Shang, Biological activities and potential health benefit effects of polysaccharides isolated from *Lycium barbarum* L, Int. J. Biol. Macromol. 54 (2013) 16–23.
[25] B. Kulczyński, A. Gramza-Michałowska, Goji berry (*Lycium barbarum*): composition and health effects – a review, in: Polish Journal of Food and Nutrition Sciences, 2016, p. 67.
[26] Y.J. Lee, Y. Ahn, O. Kwon, M.Y. Lee, C.H. Lee, S. Lee, T. Park, S.W. Kwon, J.Y. Kim, Dietary wolfberry extract modifies oxidative stress by controlling the expression of inflammatory mRNAs in overweight and hypercholesterolemic subjects: a randomized, double-blind, placebo-controlled trial, J. Agric. Food Chem. 65 (2017) 309–316.
[27] A. Masci, S. Carradori, M.A. Casadei, P. Paolicelli, S. Petralito, R. Ragno, S. Cesa, *Lycium barbarum* polysaccharides: extraction, purification, structural characterisation and evidence about hypoglycaemic and hypolipidaemic effects. A review, Food Chem. 254 (2018) 377–389.
[28] M. Protti, I. Gualandi, R. Mandrioli, S. Zappoli, D. Tonelli, L. Mercolini, Analytical profiling of selected antioxidants and total antioxidant capacity of goji (*Lycium spp.*) berries, J. Pharm. Biomed. Anal. 143 (2017) 252–260.
[29] Z.Q. Zhou, H.X. Fan, R.R. He, J. Xiao, B. Tsoi, K.H. Lan, H. Kurihara, K.F. So, X.S. Yao, H. Gao, A.O. Lycibarbarspermidines, New dicaffeoylspermidine derivatives from wolfberry, with activities against Alzheimer's disease and oxidation, J. Agric. Food Chem. 64 (2016) 2223–2237.

[30] Z.-Q. Zhou, J. Xiao, H.-X. Fan, Y. Yu, R.-R. He, X.-L. Feng, H. Kurihara, K.-F. So, X.-S. Yao, H. Gao, Polyphenols from wolfberry and their bioactivities, Food Chem. 214 (2017) 644–654.

[31] P.F. Zhu, Z. Dai, B. Wang, X. Wei, H.F. Yu, Z.R. Yan, X.D. Zhao, Y.P. Liu, X.D. Luo, The anticancer activities phenolic amides from the stem of *Lycium barbarum*, Nat. Prod. Bioprospecting 7 (2017) 421–431.

[32] R.f. Yang, C. Zhao, X. Chen, S.w. Chan, J.-y. Wu, Chemical properties and bioactivities of Goji (*Lycium barbarum*) polysaccharides extracted by different methods, J.Funct. Foods 17 (2014) 903–909.

[33] S.-H. Cho, E.-J. Park, E.-O. Kim, S.-W. Choi, Study on the hypochlolesterolemic and antioxidative effects of tyramine derivatives from the root bark of *Lycium chenese* Miller, Nut. Res. Pract. 5 (2011) 412–420.

[34] P.-C. Pan, M.-J. Cheng, C.-F. Peng, H.-Y. Huang, J.-J. Chen, I.-S. Chen, Secondary metabolites from the roots of Litsea hypophaea and their antitubercular activity, J. Nat. Prod. 73 (2010) 890–896.

[35] M. Efdi, K. Ohguchi, Y. Akao, Y. Nozawa, M. Koketsu, H. Ishihara, N-trans-feruloyltyramine as a melanin biosynthesis inhibitor, Biol. Pharm. Bull. 30 (2007) 1972–1974.

[36] S. Okombi, D. Rival, S. Bonnet, A.-M. Mariotte, E. Perrier, A. Boumendjel, Analogues of N-hydroxycinnamoylphenalkylamides as inhibitors of human melanocyte-tyrosinase, Bioorg. Med. Chem. Lett 16 (2006) 2252–2255.

[37] D.G. Lee, Y. Park, M.-R. Kim, H.J. Jung, Y.B. Seu, K.-S. Hahm, E.-R. Woo, Anti-fungal effects of phenolic amides isolated from the root bark of *Lycium chinense*, Biotechnol. Lett. 26 (2004) 1125–1130.

[38] H. Siddiqui, M.A. Bashir, K. Javaid, A. Nizamani, H. Bano, S. Yousuf, A.-u. Rahman, M.I. Choudhary, Ultrasonic synthesis of tyramine derivatives as novel inhibitors of α-glucosidase in vitro, J. Enzym. Inhib. Med. Chem. 31 (2016) 1392–1403.

[39] D. Seebach, T.L. Sommerfeld, Q. Jiang, L.M. Venanzi, Preparation of Oxazolidine-Containing Peptides: unusual effects in RhIII-catalyzed acetalizations of aldehydes with urethane-protected serine and threonine esters and with dipeptides containing serine or threonine residues at the N-terminus, Helv. Chim. Acta 77 (1994) 1313–1330.

[40] S.-H. Han, H.-H. Lee, I.-S. Lee, Y.-H. Moon, E.-R. Woo, A new phenolic amide from *Lycium chinense* Miller, Arch Pharm. Res. (Seoul) 25 (2002) 433–437.

[41] M.H. Yang, Y. Vasquez, Z. Ali, I.A. Khan, S.I. Khan, Constituents from Terminalia species increase PPARα and PPARγ levels and stimulate glucose uptake without enhancing adipocyte differentiation, J. Ethnopharmacol. 149 (2013) 490–498.

[42] P.A. Elzahhar, R. Alaaeddine, T.M. Ibrahim, R. Nassra, A. Ismail, B.S.K. Chua, R.L. Frkic, J.B. Bruning, N. Wallner, T. Knape, A. von Knethen, H. Labib, A.F. El-Yazbi, A.S.F. Belal, Shooting three inflammatory targets with a single bullet: novel multi-targeting anti-inflammatory glitazones, Eur. J. Med. Chem. 167 (2019) 562–582.

[43] Schrödinger, in: Release 2015-2: Maestro, Version 10.3, Schrödinger, LLC, New York, NY, 2015, 2015.

[44] J. Zhao, S.I. Khan, M. Wang, Y. Vasquez, M.H. Yang, B. Avula, Y.-H. Wang, C. Avonto, T.J. Smillie, I.A. Khan, Octulosonic acid derivatives from roman chamomile (Chamaemelum Nobile) with activities against inflammation and metabolic disorder, J. Nat. Prod. 77 (2014) 509–515.

[45] J.M. do Carmo, A.A. da Silva, Z. Cai, S. Lin, J.H. Dubinion, J.E. Hall, Control of blood pressure, appetite, and glucose by leptin in mice lacking leptin receptors in proopiomelanocortin neurons, Hypertension 57 (2011) 918–926.

[46] J.M. do Carmo, A.A. da Silva, P.O. Sessums, S.H. Ebaady, B.R. Pace, J.S. Rushing, M.T. Davis, J.E. Hall, Role of Shp2 in forebrain neurons in regulating metabolic and cardiovascular functions and responses to leptin, Int. J. Obes. 38 (2014) 775–783.